A microscopic description and ultrastructural characterization of *Dientamoeba fragilis:* an emerging cause of human enteric disease

Gouri R. Banik [a, b, c], Debra Birch [d], Damien Stark [a,c] and John T. Ellis [b,c]*

[a]*Division of Microbiology, SydPath, St. Vincent's Hospital, Darlinghurst, Australia*

[b]*University of Technology Sydney, i3 Institute, Broadway, Australia*

[c]*University of Technology Sydney, School of Medical and Molecular Biosciences, Broadway, Australia*

[d]*Department of Biological Sciences, Macquarie University, Sydney, New South Wales, Australia*

*Corresponding author: School of Medical and Molecular Biosciences, University of Technology, Sydney, P.O. Box 123, Broadway, NSW 2065, Australia, Tel: 61 (02) 95144161 Fax: 61 (02) 95144003, E-mail: John.Ellis@uts.edu.au

Abstract

Dientamoeba fragilis is a pathogenic trichomonad found in the gastrointestinal tract of humans and is implicated as a cause of diarrhoea. Despite its discovery over a century ago, there has been no recent thorough description of this parasite by microscopy. SEM, TEM, confocal and light microscopy were therefore used to characterize *D. fragilis* populations growing in xenic culture. Two different populations- smooth and ruffled cells were identifiable by SEM. No flagella, pelta structures, undulating membrane or pseudocyst-like forms were present. The organelles in *D. fragilis* were analysed by TEM; like *Trichomonas* and *Histomonas*, *D. fragilis* contains hydrogenosomes that presumably represent the site of anaerobic respiration. The nuclear morphology of *D. fragilis* trophozoites grown *in vitro* and trophozoites from clinical isolates were also compared by confocal microscopy and light microscopy. The majority of cells grown in culture were mononucleate while most cells in permanent stained fecal smears were binucleate. The two nuclei of *D. fragilis* are morphologically indistinguishable and contain equivalent amounts of DNA as determined by DAPI staining. The approximate cell and nuclear volume of four isolates of *D. fragilis* were measured and shown to be comparable to other trichomonads. In addition, the discovery of a Virus-Like Particle (VLP) is also reported for the first time in *D. fragilis*. This study therefore provides extensive and novel details of the ultrastructure of a neglected protozoan parasite that is an emerging cause of human disease.

Key words: *Dientamoeba fragilis*; Electron microscopy; Ultrastructure; Trichomonad; Dientamoebiasis; Virus-like particle.

1. Introduction

Dientamoeba fragilis is a trichomonad protozoan that belongs to the Parabasalia group (Gerbod et al., 2002; Ohkuma et al., 2005; Cepicka et al., 2010). It is found in the gastrointestinal tract of humans where it is associated with chronic gastrointestinal disease and has worldwide distribution (Stark et al., 2010a; Stark et al., 2010b; Barratt et al., 2011a). It is almost a century since *D. fragilis* was first described by Jepps & Dobell who initially classified it as an amoeba (Jepps and Dobell, 1918; Johnson et al., 2004). Studies related to molecular phylogenetics (Delgado-Viscogliosi et al., 2000; Gerbod et al., 2001) and morphological analysis (Camp et al., 1974) then confirmed that *D. fragilis* was a trichomonad that has no flagella in the trophozoite stage of its life cycle. The complete life cycle of this parasite has not yet been fully determined and the trophozoite is the only known stage (Stark et al., 2008; Barratt et al., 2011b). Morphologically, *D. fragilis* is a single-celled pleomorphic trophozoite typically ranging from 5 to 15 μm in diameter that contains one to four nuclei (Sawangjaroen et al., 1993; Johnson et al., 2004; Stark et al., 2006). The presence of four or five nuclei is also described (Dobell, 1940; Wenrich, 1944a; Moody and Fleck., 1985). Characteristically high percentages of *D. fragilis* trophozoites are binucleate with a large fragmented central karyosome without peripheral chromatin observed previously from stained feces (Stark et al., 2006). It is not possible to see nuclear structure in an unstained preparation (Windsor and Johnson, 1999; Stark et al., 2008). Moreover, the nuclei of *D. fragilis* are not visible in saline or iodine preparations, although food vacuoles or inclusions may be seen (Johnson et al., 2004). No cyst stages have been reported yet for this parasite (Windsor et al., 2003; Stark et al., 2006; Barratt et al., 2011b).

One of the unusual features of *D. fragilis* is the presence of two nuclei (binucleate forms) (Johnson et al., 2004; Stark et al., 2010a). Previous studies reported that another protozoan parasite *Giardia lamblia* also has two equal sized nuclei which are equivalent with respect to the amount of DNA harboured in each and replicate at approximately the same time (Wiesehahn et al., 1984; Kabnick and Peattie, 1990; Cerva and Nohýnková, 1992; Svärd et al., 2003; Benchimol, 2004b). This organism represents one of the earliest diverging lineages of eukaryotes (Adam, 2001; Svärd et al., 2003). There are other protozoans which have been studied in more details with two or more nuclei. These includes the ciliates, *Tetrahymena* and *Paramecium* (Southern, 1975; Prescott, 1994); *Tetrahymena* has one diploid micronucleus, and *Paramecium* has two equal, diploid micronuclei (Jahn and Klobutcher, 2002). *Dientamoeba fragilis* was reported as typically binucleate almost a century ago (Jepps and Dobell, 1918; Craig, 1926) but the nuclei have not been studied with regard to DNA content or transcriptional activity. It is important to determine whether the two nuclei of *D. fragilis* are structurally and functionally identical as well as to understand the evolutionary, physiological and genetic significance of these two physically separate, but equal-sized, nuclei.

To our knowledge, only a few studies have described the ultrastructure of *D. fragilis* by TEM (transmission electron microscopy) (Camp et al., 1974; Ockert and Schneider, 1974; Silard et al., 1984; Silard and Burghelea, 1986). Camp et al. (1974) published a study of the binucleate stage of *D. fragilis* (strain Bi/pa) and the ultrastructure of mononucleate stages (CE stain of *D. fragilis*) were described by Silard et al. (1984). New studies need to be undertaken due to recent advances in the cell biology of trichomonads. For example, hydrogenosomes are known features of a trichomonad cell

but they have yet to be described for *D. fragilis*. Until today, there are also no studies which report the SEM (scanning electron microscopy) characteristics of *D. fragilis.*

This study aimed to describe and characterize *D. fragilis* by different microscopy methods in order to define cell size, shape, surface organization, ultrastructure of different organelles including nuclei numbers. SEM, TEM, confocal and light microscopy was used to examine these characteristics and the current results are reported here. The ultrastructure of four isolates of *D. fragilis* is described. This study is the first SEM analysis of *D. fragilis* which contributes to the understanding of the surface biology of this parasite. This study provides new insights into the cell biology and many novel morphological aspects of *D. fragilis* and thus allows better understanding of the main aspects of its cell biology.

2. Materials and methods

2.1. Culture of D. fragilis trophozoites

Four *Dientamoeba fragilis* isolates (isolate 1, isolate 2, isolate 3 and isolate 4) used in this study were previously described (Barratt et al., 2010). All *D. fragilis* isolates were grown anaerobically at 37°C in tissue culture flasks with anaerobic or microaerophilic gas packs (Oxoid AnaeroGen^{TM} AN0035A) in an anaerobic jar (BD GaspakTM EZ). Loeffler's serum slopes contain heat-inactivated horse serum (Bovogen), glucose (Sigma) and nutrient broth (Sigma) in distilled water and were prepared as previously described (Barratt et al., 2010). Fifteen ml of Loefflers media were poured into a 50 ml culture flask (Nunc^{TM} 156367) sloped and inspissated in an 85°C drying oven until the serum slopes solidified. Finally, the media was completed by addition of 15 ml PBS (Sigma) and supplemented with 3-5 mg of sterilized rich starch (Sigma S7260).

2.2. Scanning electron microscopy

Cell suspensions of 1.0X10^{6} trophozoites/ ml were collected after 48 h of subculture and concentrated into 1.5 ml Eppendorf tubes (100µl) which were then centrifuged at 1000g for 5 min. The supernatant was removed and cell pellets were fixed in 5% (v/v) glutaraldehyde in phosphate buffered solution (0.1M, pH 7.2) overnight at room temperature. The cells were then washed three times for 10 min each wash with PBS. To prepare cells for SEM, coverslips (12 mm X 12 mm) were coated with 0.1% ethylene imine polymer solution (Fluka, Switzerland). Cell suspensions (20µl) from each isolate were added to the coverslips and cells were allowed to adhere for 10 min at room temperature. The adherent cells were then washed in buffer three times for 10 min each wash (0.1M Phosphate Buffer, pH 7.2) and post-fixed in 1% osmium tetroxide (OsO4) in

0.1M phosphate buffer solution (pH 7.2) for 1h. Following post-fixation, the samples were washed in the same buffer triplicate for 5 min each and then dehydrated through a graded series of ethanol of 30%, 50%, 70%, 90% , 95% and 100%, 10 min each step. One set of samples were transferred to a critical point dryer (Emitech K850) and the other set dehydrated using HMDS (hexamethyldisilazane, Sigma). The coverslips were mounted on aluminum stubs and sputter coated with gold (Emitech K550). Observations were carried out using a JEOL 6480 LA scanning electron microscope. All SEM materials were supplied from ProScitech, Australia.

2.3. Investigation on pseudocyst-like stages formation by SEM

Previous reports noted that cooling of cultures of trichomonads from their normal growth temperature of 37^0C to below 16^0C (Granger et al., 2000), 4°C for *Histomonas* (Zaragatzki et al., 2010) or 20°C for *Monocercomonas sp.* (Borges et al., 2007) can trigger pseudocyst formation. To investigate the effects of temperature on the life cycle of *D. fragilis*, trophozoites were incubated at 4°C, 16°C and 20°C for 48h. The initial trophozoite density was $1.0X10^6$ trophozoites/ml, and the trophozoites were counted in a hemocytometer every 24 h. All experiments were performed in triplicate. Controls were incubated under normal *in vitro* cultivation at 37°C. Post incubation cells were fixed and processed for SEM as above.

2.4. Transmission electron microscopy

Cell suspensions ($1.0X10^6$ trophozoites/ml) from four *D. fragilis* isolates were collected after 48 h of subculture into 1.5ml Eppendorf tubes (100µl) and were then centrifuged at

1000g for 5 min. The supernatant was removed and cell pellets were fixed in 5% (v/v) glutaraldehyde in phosphate buffered solution (0.1M, pH 7.2), overnight at room temperature. Fixed cells were centrifuged at 5000 rpm for 5 min, the fixative was removed and fresh buffer added. The buffer washing step was repeated three times for 15 min each wash. Cell pellets were embedded in 1% low melt agarose (J.T. Baker inc. Phillipsburg, USA). The agar blocks were cut into 1 mm cubes, transferred to glass vials and post-fixed in 1% osmium tetroxide (OsO4) in 0.1 M phosphate buffered solution for 1 h at room temperature. Following post-fixation, the samples were washed in distilled water triplicate for 5 min each and immersed in 2% aqueous uranyl acetate for 30 min. The pellets were dehydrated through a graded series of ethanol (50% - 100%), infiltrated and subsequently embedded in London White Resin (L.R.White). Semi-thin and ultra-thin sections were cut using a Reichert ultramicrotome (Ultracut, Leica Microsystems, Germany). Semi-thin sections (1 μm thickness) were stained with 1% methylene blue and observed by transmitted light microscopy (Olympus BH2). Ultra-thin sections (70 nm) were mounted onto Pioloform coated, 300 mesh, thin bar copper grids, stained with saturated aqueous uranyl acetate (7.7%) for 30 min and Reynold's lead citrate for 4 min. Ultrathin sections were examined using a Philips CM10 transmission electron microscope (Eindhoven, the Netherlands). All TEM materials were supplied from ProScitech, Australia.

2.5. Nuclei, cell cytoplasm and cell membrane staining of Dientamoeba fragilis

2.5.1. Nuclear staining with DAPI

Dientamoeba fragilis in the logarithmic phase of growth and exhibiting more than 95% of viability were collected by centrifugation at 1000g for 5 min. The cell pellets were washed by PBS and initial trophozoite density was 1.0×10^6 trophozoites/ml (as counted in a hemocytometer). For DAPI staining, all *D. fragilis* isolates were fixed in sodium acetate acetic acid formalin (SAF) at a 1:1 ratio for 3 to 4h. Fixed cells were washed with isotonic saline (0.9% NaCl) two times at 500g for 5 min. After washing, the cells were centrifuged at 1000g for 5 min and resuspended in a minimum amount of saline. A drop of the cell suspension was applied to a microscope slide which was then mixed with a drop of 0.5% albumin (Mayer's Albumin solution, Fronine, 2604029) and spread over the slide to create a smear. The slides were allowed to air dry for about 3-4h to adhere the cells onto the slides. The fixed cells were stained with 1 ug/ml DAPI [4′, 6-diamidino-2-phenylindole, dilactate (DAPI, dilactate), Molecular Probes ™] in the dark for 15 min at room temperature. The cells were rinsed carefully with PBS to remove unbound dye. Excess liquid was removed from the slide by gently blotting around the sample with an absorbent tissue. A glass coverslip was placed on the slide and the edges sealed with wax or nail polish. DAPI stained smears were then viewed under a Laser Scanning Confocal Fluorescence Microscope (Nikon A1).

2.5.2. Nile Red staining

Cultured trophozoites were fixed in SAF solution and microscopic slides were processed for DAPI staining as above. Stock solutions of Nile Red (9-diethylamino-5H-benzo[a]phenoxazine-5-one) (Sigma) (1,000 µg/ml) were prepared in acetone and stored protected from light. Nile Red was added directly to the trophozoite preparation at l: 100

dilution. Initially, cells were stained with DAPI and then immediately stained with Nile Red. The slides were incubated at room temperature for a minimum of 10-15 min. Excess dye was removed by brief rinsing in PBS. A coverslip was added and the samples were examined using a Laser Scanning Confocal Fluorescence Microscope (Nikon A1). The suspension medium did not contain serum or albumin since this was found to act as a sink to draw Nile Red out of the cells.

2.5.3. Permanent stained smears

Human stool specimens were fixed in SAF solution and stained with a modified iron-haematoxylin stain (Fronine, Australia) according to the manufacturer's recommendations. All stained smears were examined by oil-immersion microscopy at 1000X magnification. Photographs were taken using Olympus DP70 photo microscope connected to a camera (Leica DC 300F) at magnification 100x DiC (Differential Interference Contrast). Cell diameters were measured using Image Pro Express Software.

2.5.4. Photometry and data analysis

All SEM and TEM images were analysed and measured quantitatively by using ImageJ Software (1.44). The confocal fluorescence microscope equipped with a filter for DAPI analysis (laser: excitation 400 nm and emission 450-475 nm) was used. Cells were photographed at magnification 100 x DiC with the pinhole open. Mononucleate and binucleate cells were viewed as 3D focal plane (X-Y and Y-Z) using Z- Stack optical sectioning during scanning by confocal microscopy.

The DAPI fluorescence emitted from each nucleus was quantitated photometrically as previously described (Kabnick and Peattie, 1990). The dimension (length and width) of each cell was measured by using 3D measurement tools in the NIS Viewer Software.

2.5.5. Estimation of cell and nucleus volume

Cell dimensions as well as approximate cell volume were measured for all four isolates of *D. fragilis*. All four *D. fragilis* isolates were attached to microscope slides that were fixed with SAF solution (as described for DAPI staining method) and observed using a combination of differential interference contrast illumination and fluorescence of DAPI stained in confocal microscope (Nikon A1). Photographs were taken of fifty non-dividing cells of each *D. fragilis* isolate. The dimension of cells and nuclei were made using NIS Viewer Software. Approximate cell and nucleus volumes (V) were calculated according to the formula $V = 3/4\pi ab2$ where "*a*" is the cell length, and "*b*" is the cell width as previously described (Zubácová et al., 2008). Standard deviation of cell length and width of 50 non-dividing cells from each isolate were determined.

3. Results

3.1. Characterization of cell surfaces of D. fragilis

The external structures of four isolates of *D. fragilis* studied by SEM are described. Firstly, the cell shapes and sizes of four clinical isolates of *D. fragilis* trophozoite (Fig. 1) were examined. By SEM, the cell shape of the four isolates of *D. fragilis* varies from spherical to ovoidal, sometimes amoeboid ranging in size from approximately 4-10μm. There was no flagella, undulating membrane, axostyle–pelta structures. Other typical characteristics of *D. fragilis* observed were bacteria adhered to *D. fragilis* surfaces and phagocytosis of bacteria and rice starch (Fig. 2).

3.2. Phagocytic activity of D. fragilis

It was observed by SEM that trophozoites in fresh cultures exhibited phagocytosis (Fig. 2)**.** The attachment of bacteria to the cell surface of the parasite was observed frequently (Fig. 2C)**.** *Dientamoeba fragilis* constantly changes its shape, engulfs bacteria and rice starch available from the culture medium. It also exhibits an amoeboid morphology during the internalization of food particles. A variety of motile forms of *D. fragilis* were observed. Mostly two forms of phagocytosis were observed: a ‘sinking’ process without any apparent participation of plasma membrane extensions (Fig. 2A, B), and the classical phagocytosis where pseudopodia were extended by amoeboid movement toward the target food particles (Fig. 2D). Interestingly, *D. fragilis* was also able to phagocytose even when undergoing the division process (Fig. 3C, D).

3.3. Two different populations of D. fragilis

Under the SEM, two types of *D. fragilis* populations were classified based on cell surface structure: ruffled cells and smooth cells (Fig. 1II, E & F). To examine the relative numbers of both cell types, a time interval experiment was performed by collecting cells at different time points of culture (6h, 12h, 24h, 32h, 48h, and 72 h). Ruffled cells were more common than smooth cells. During the time interval, from 6- 48h, 90% of the cells were ruffled while at 72h, 30% cells appeared to be smooth.

3.4. Growth stages of D. fragilis

In addition, different stages of development and activities of *D. fragilis* trophozoites were observed during this experiment (Fig. 3). Phagocytosis was the most common phenomena observed in most of the cells at 6h and 12h. A number of trophozoites divided by binary fission which occurred by the simple constriction of the cell body (Fig. 3C, D). Ninety eight percent (98%) of trophozoites were considered to have finished their binary fission between 32- 48h. Because of the lack of nutrient in the cell culture medium at 72 h, trophozoies probably were approaching stationary phase at this time point (Fig 3F)**.**

3.5. Pseudocyst –like stage formation

This experimental system was used for the study of rapid and reversible formation of pseudocysts-like stages in culture in response to unfavoured culture conditions. To induce encystation, *D. fragilis* was cultivated for 48 h at either 4°C, 16°C and 20°C and the populations analyzed by SEM. The comparison showed variable size differences between

trophozoites grown under the different conditions. Nearly all of the cells appeared nonviable, damaged and smaller in size than normal cells grown at 37 ^{o}C. The cell wall surface appeared to be non-intact under these adverse conditions. It was concluded that pseudocysts were not present in these cultures.

3.6. Transmission electron microscopy: ultrastructural observations on four isolates of D. fragilis

The morphological characteristics, such as cell shape, size, ultrastructure of different organelles including nuclei numbers of four isolates of *D. fragilis* collected from *in vitro* cultures was examined (Fig. 4A, B, C) (Table 3). Usually *D. fragilis* has a spherical or oval shape with a granular, vacuolated cytoplasm and some cells are amoeboid. *Dientamoeba fragilis* exhibited different motile forms with visible pseudopodia (Fig. 4D). The cell size varies from 3 to 15 μm and nucleus diameter from 0.8 to 3.5 μm in all four isolates. The fine ultrastructure of 100 cells (25 cells from each isolate) were examined in detail and more than 80% of cells from each isolate (isolate 1: mononucleate cell 96%, binucleate 4%; isolate 2: mononucleate cell 84%, binucleate 16%; isolate 3: mononucleate cell 92%, binucleate 8%, isolate 4: mononucleate cell 92%, binucleate 8%) were mononucleate. A small number of trinucleate and anucleate cells were also observed.

3.6.1. Nucleus

The size of the nucleus in mononucleated trophozoites varied from 0.86-3.52 μm and in binucleated cells from 1.12-2.06 μm. A number of mononucleated cells appeared to have

dividing nuclei and nucleoli (Fig 5. C, D) and were larger than binucleated nuclei. The nucleus in nondividing mononucleate and binucleate cells was spherical but some oval or irregularly shaped nuclei were observed. The nuclear envelope consists of a double membrane containing numerous nuclear pores (Fig. 5A, arrowed)**.** The nuclear matrix is filamentous and contains electron dense material.

The *D. fragilis* nucleus is normally seen in the central region of the cell. Both mononucleate and binucleate trophozoites have fragmented nuclei and usually contain two to eight chromatin bodies (Fig. 5A) without peripheral chromatin. Chromatin bodies were found scattered throughout the nucleus and varied in size. The nucleolus is mainly located in the periphery of the nucleus not at the polar center and appears as a rounded structure. It consists of a dense fibrillar component and is not surrounded by a membrane. There appears to be only one nucleoli per nucleus (excluding the dividing stages) (Fig. 5C).

The mononucleate form of *D. fragilis* is the predominant stage observed in *in vitro* cultures. A number of cells appeared to be dividing by binary fission (Fig. 5B). The mechanism of this division was the simple constriction of the cell body. Nuclear division was observed only in mononucleated trophozoites. The extranuclear spindle was found between the nuclei in binucleate cells, emanating from the polar complex adjacent to one of the nuclei (Fig. 5B, arrow)**.** It extended between the two nuclei, each nucleus surrounded by an envelope with nuclear pores. The spindle microtubules originated in pairs and non periodic structures. About 20-30 microtubules are often seen as clusters and occasionally in order. Different types of microtubules were observed throughout the cell: pole-to-pole, pole-to-nucleus, and pole-to-cytosol microtubules. The spindle microtubules

are assembled from a attractophore (V-shaped center) which is located underneath the basal bodies (Fig. 8A). No kinetosomes or centriole like organelles have been found in the polar complexes or elsewhere in the organism.

3.6.2. The Golgi complex

A well-developed Golgi complex was found in all isolates of *D. fragilis* (Fig. 6A). The Golgi complex was observed as a vesicular structure generally in the perinuclear area and in close proximity to the endoplasmic reticulum. Golgi vesicles were also seen in the area between branching bundles of microtubules. The Golgi of *D. fragilis* has the following characteristics: It is a single and very prominent structure, it is about 450 nm long and it has about 7-10 cisternae. The Golgi complex appears to be more developed in the mononucleated cells. On the other hand, in binucleated cells, the Golgi complex does not appear in an organized form and was mostly fragmented. Numerous circular vesicles can be seen in proximity to the Golgi complex.

3.6.3. Endoplasmic Reticulum (ER)

Both smooth and rough endoplasmic reticulums were well-developed in the mononucleate and binucleate *D. fragilis* trophozoite (Fig. 6B, C). It was clearly observed in all four isolates. Rough ER was more frequently found in the cytoplasm of mononucleated cells. The ER is also clearly seen around the nucleus and sometimes closely associated with the hydrogenosomes, food vacuoles and microtubules.

3.6.4. Hydrogenosomes

TEM showed the presence of hydrogenosomes in *D. fragilis* while mitochondria and peroxisomes were not observed. Hydrogenosomes are double layered membrane bound electron-dense organelles located in the cytoplasm of *D. fragilis*. These were found in all four *D. fragilis* isolates used in this study, sizes ranging from 0.12-0.83µm and in number varying from 5 to 15 (Fig. 6D, E)**.** This organelle was spherical or oval shaped or sometimes slightly elongated in structure. The membrane of the hydrogenosome is smooth, while the matrix of the hydrogenosome is homogeneously granular. Hydrogenosomes with a variety of electron densities were present. They possess a peripheral vesicle, although it is clear that the shape of these organelles largely depends on the plane of section. They are usually associated with cytoplasmic inclusions and with digestive vacuoles. Close proximity, and even continuity, between the endoplasmic reticulum and hydrogenosomes was observed.

3.6.5. Digestive vacuole (DV) / Food vacuole

Digestive or food vacuoles (DV) were commonly found throughout the cytoplasm and may contain bacteria, rice starch and myelin configurations (Fig. 7A, B). Their size varies from 0.59- 4.2 µm. The numbers of DV were seen to vary from 1-10 in all four isolates. Rice starch was comparatively small and observed throughout the cells. A number of digestive vacuoles contained rice starch and bacteria, clearly recognizable in the early stages of digestion. *Dientamoeba fragilis* feeds by phagocytosis (Fig. 7C, E), and waste products are released from the digestive vacuoles by exocytosis (Fig. 7F)**.** It was also observed that *Dientamoeba* trophozoites are bound by a double layered cell membrane (Fig. 8F)**.** This membrane does not give rise to the cell mouth (micropore, cytostome) but

appears to form pinocytotic vesicles and small food vacuoles, which engorge material from the culture media.

3.6.6. Lysosomes

Lysosomes were present in different sizes (0.50- 2 μm) mainly in the posterior region of the cell in close proximity to the cell membrane (Fig. 6F)**.** They were also seen in close proximity to digestive vacuoles and other cytoplasmic organelles. The internalized bacteria and rice starch were digested in lysosomes.

3.6.7. Cytoplasm and other cytoplasmic inclusions

The cytoplasm contains large deposits of glycogen, electron dense materials and ribosomes and is surrounded by a double layered cell membrane. During phagocytosis, invagination appears in the cytoplasm and gradually its edges are drawn together (Fig. 7C). Glycogen granules are distributed throughout the cytoplasm of different sizes (Fig. 4A). Rough endoplasmic reticulum is less frequently identifiable and not concentrated in the perinuclear region. Electron dense materials (Fig. 8F) were scattered throughout the cytoplasm. The central zone of some cells was completely filled with the electron dense materials.

3.6.8. The basal body structure: Axostyle -Costa

The basal body structure of *Dientamoeba* contains an axostyle and a costa. The pelta structures or flagella were not found. Multiple ribbons of microtubules formed the axostyle, which runs from the basal bodies to the cell tip (Fig. 8A, arrow) and outlines the

axis of cell. The axostyle were usually found in the anterior region of the cell near the cell membrane. Axostyle was also observed in the middle of cells adjacent to the nucleus. The anterior portion of the axostyle is wider than the posterior region. It is also associated with other organelles such as endoplasmic reticulum, hydrogenosomes and sigmoid filaments. It is noteworthy to mention that, the complete structure of the axostyle is very seldom seen. The appearance of the axostyle under TEM is very dependent on the plane of section. The costa, another basal body cytoskeletal structure, is periodic and proteinaceous and formed by a microtubular sheet. Costa was frequently found near the cell surface and in the middle region of cell (Fig. 8D). It comprises a complex array of filaments and often makes contact with a network of other filaments present in the cytoplasm.

3.6.9. Parabasal filament

Parabasal filament (PF) is another component of the basal body cytoskeleton and was found in all isolates of *D. fragilis*. It appears as a microfibrillar strand linked to the basal bodies. This structure is seen as singular (Fig. 8E) or in a cluster (Fig. 8B), close to the nucleus and Golgi complex and extends laterally to the external surface of the atractophores. Clusters of the parabasal apparatus were frequently observed in all isolates often underlying a V-shaped structure (attractophore) (Fig. 8A). The Parabasal filament is composed of approximately 30 to 40 hairy-like segments. Occasionally, it is composed of two bundles, one bundle appears at some distance from the nucleus, whereas the other is juxtanuclear and is often seen in a groove of the nuclear envelope.

3.6.10. Phagocytosis

A number of trophozoites showed irregularly protruding pseudopodia by TEM. An amoeboid form of *D. fragilis* was frequently observed (Fig. 4D). *Dientamoeba fragilis* frequently changes its shape when it is engulfing bacteria or rice starch (Fig. 7C, E). TEM observations showed clearly that phagocytosis is initiated by the binding of bacteria or rice starch on surface of *D. fragilis* cell. These interactions trigger cytoskeletal changes that lead to pseudopod extensions, engulfing bacteria or rice starch. Finally phagosomes were formed (Fig. 7D) which allow to digest the food particles. A convoluted plasmalemma (Fig. 7E, arrow) was occasionally observed, probably associated with the early stages of phagocytosis forming a 'phagocytic cup' around bacteria or rice starch.

3.6.11. Virus - like particle (VLP) in *Dientamoeba fragilis*

Virus- Like particles (VLPs) were seen frequently inside the cytoplasm of trophozoites by TEM during ultrastructural analysis (Fig. 9). VLP sizes varied between 40 to 200 nm. Their most common shape was spherical, enclosing a dense core, a middle electron-lucent layer and an outer coat.

3.7. Confocal and light microscopy observations

Dientamoeba fragilis cells and nuclei from *in vitro* cultured condition were studied by confocal microscopy and in permanently stained fecal smears by light microscopy. In

most experiments, cells were fixed onto microscopic slides. This provided a constant, known orientation of the nuclei in all cells in these experiments.

3.7.1. The two nuclei contain equal amounts of DNA

To determine whether the two nuclei of *D. fragilis* contain equivalent amounts of DNA, *D. fragilis* trophozoites were stained with DAPI, an agent that binds specifically and strongly to DNA independent of its sequence. When DAPI becomes intercalated with nuclear DNA, a bright blue fluorescence is emitted (Fig. 11). The fluorescence emitted from each nucleus was quantitated photometrically by readings made through a microscopic aperture. The nuclei of all four isolates of *D. fragilis* were examined. There was no apparent difference in the DNA content of nuclei in cells containing two nuclei i.e. DNA content of both nuclei is equal (Table 1)**.**

3.7.2. Comparison of *D. fragilis* nuclei from *in vitro* culture & permanent stained smears

Sixty percent (60 %) of trophozoites in permanently stained fecal smears were binucleate, 30% were mononucleate and 9% were anucleated (Fig. 10). In contrast, 70% of *in vitro* cultured *D. fragilis* trophozoites were mononucleate, 29% were binucleate and 1% was anucleate as determined by confocal microscopy. However one cell containing three nuclei was found in permanently stained smears (Fig. 10C) and very few trophozoites with three nuclei were observed in cultures (data not shown). The cells containing three nuclei observed in cultures seem to be a dividing form. For this reason this nuclei number was not included with the data counting for comparison. Light microscopy and confocal microscopy observation showed that *D. fragilis* trophozoites appeared to have a wide

variation in shapes and sizes. From stained smears, *D. fragilis* were found from 4 to16 µm. The size range of cultured *D. fragilis* trophozoites was from 5 to 25 µm and the nuclei of *D. fragilis* were seen from 0.5 to 3.5 µm for all four isolates. *Dientamoeba fragilis* usually appeared rounded but different morphology was also observed such as oval shaped, ameboid, rod shaped and also phagocytic stages were seen (Fig. 13D). *Dientamoeba fragilis* moves by using leaf-like pseudopodia which are irregularly lobed found in cultured conditions. In addition, typical fragmented nuclei were also found in permanent stained smears.

3.7.3. Comparison of mononucleate and binucleate *D. fragilis* trophozoites at different time intervals of cultures

The ratio of mononucleate and binucleate cell numbers during different growth stages in culture media was determined (Fig. 12). A total of 500 cells from isolate 1 were stained with DAPI and analyzed at different time intervals (6h, 12h, 24h, 48h, and 72 h) by confocal microscopy. Approximately 100 non-dividing DAPI stained cells were counted at each time point. Eighty three percent (83%) of cells were found as mononucleate and 17% of the trophozoites were binucleate after 6 h. The number of binucleate trophozoites increased at 24h and 48h time point of *in vitro* growth. During counting dividing cells were omitted. It appeared that *D. fragilis* nuclei divided non-synchronously during binary fission. At 6 h and 12 h trophozoites were generally smaller in size (5 µm -10 µm).

3.7.4. Cell and nuclear volume of *D. fragilis*

The cell and nuclear dimensions of *D. fragilis* were obtained from Nile Red stained *D. fragilis* and DAPI stained nuclei (Fig. 13A, B, C). Finally, the approximate volumes of *D. fragilis* cells as well as nuclei were calculated (Table 2)**.** These steps were repeated for each of the four isolates of *D. fragilis*. There was no significant difference between the cell and nucleus volume between the four isolates.

4. Discussion

This is the first electron microscopy study in forty years to examine the ultrastructure of *D. fragilis*. Even though *D. fragilis* is recognised as a significant human pathogen (Stark et al., 2010b; Barratt et al., 2011a), most of the microscopic observations of *D. fragilis* date back to the early and mid-1900s (Johnson et al., 2004) and therefore may represent inappropriate descriptions of this parasite. Comparing with other common trichomonads such as *Trichomonas vaginalis* (Benchimol et al., 2002; Benchimol, 2004a; Chen et al., 2004), *Tritrichomonas foetus* (Benchimol et al., 1993; Benchimol et al., 1996; Benchimol, 2000), *Trichomonas gallinae* (Mehlhorn et al., 2009) and *Histomonas meleagridis* (Mielewczik et al., 2008; Munsch et al., 2009; Zaragatzki et al., 2010) very little information is available about the biology of this organism. The present study deals with four different *D. fragilis* isolates which were cultivated *in vitro*. Different microscopy methods were performed to characterize their surface structures, fine ultrastructure and details observations on nucleus characteristics of this neglected protozoan.

In the last few years, several studies had provided information on morphology of other protozoan parasites based on SEM. *Trichomonas vaginalis* (Ovcinnikov et al., 1975; Kurnatowska and Hajdukiewicz, 1977; Warton and Honigberg, 1979; Benchimol, 2004a), *Tritrichomonas foetus* (Warton and Honigberg, 1979), *Pentatrichomonas hominis* (Warton and Honigberg, 1979) and *Trichomitus batrachorum* (Honigberg et al., 1972), *Hypotrichomonas Acosta* (Warton and Honigberg, 1979) have all been studied in detail. Much has been learned about the structure of *Trichomonas gallinae*, first by light microscopy (Stabler, 1941, 1954; Abraham and Honigberg, 1964; Honigberg, 1978), and

then by TEM (Mattern et al., 1967; Benchimol et al., 1997) and SEM (Kietzmann GE, 1993; Tasca and De Carli, 2003; Mehlhorn et al., 2009). In order to provide a detailed description of *D. fragilis* a range of microscopic techniques were used and the results are reported here.

In the present report we studied four isolates of *D. fragilis* by SEM which permits the examination of intact *D. fragilis* and their surface structure details. The SEM observations showed that two types of populations were present based on cell surface structures: ruffled and smooth cells, with the number of ruffled cells being significantly higher in all isolates. Ruffled cells are also observed for other trichomonads (Ovcinnikov et al., 1975; Tasca and De Carli, 2003; Borges et al., 2004). It is unknown if the appearance of the cell surface is important and what biological differences it represents. Clearly it represents a significant change in the trophozoite structure and presumably its physiology.

Other studies have described more rounded cells which were reported as pseudocyst-like stages in trichomonads (Tasca and De Carli, 2003; Tasca and De Carli, 2007). The possibility of pseudocysts-like stages formation in *D. fragilis* was investigated by SEM. *Dientamoeba fragilis* grows in a relatively warm environment (37^0C - 42^0C), and cooling might provide a rapid signal that would trigger changes in the trophozoite to protect against the adverse environmental growth conditions. *Dientamoeba fragilis* trophozoites were cultivated under different adverse temperatures and the trophozoites were observed by SEM. As *D. fragilis* do not contain flagella and undulating membranes like other trichomonads, it is difficult to investigate the formation of pseudocysts under adverse conditions. Most of the other trichomonad studies described the presence of more

spherical forms as probably pseudocysts (Granger et al., 2000; Tasca and De Carli, 2003; Borges et al., 2007; Tasca and De Carli, 2007). In this study no evidence was found for the presence of spherical pseudocyst-like stages under these experimental adverse conditions.

Different growth stages of *D. fragilis* were observed during the course of this study. Interestingly, different activities such as amoeboid movement, phagocytosis and bacterial adhesion to trophozoite surfaces were also observed clearly. No flagella structures, undulating membrane and axostyle were found by SEM. Even though phagocytosis is an essential phenomenon in *D. fragilis*, the details of the phagocytic activity of this parasite has not yet been elucidated. In this study, the *in vitro* capacity of *D. fragilis* to phagocytose (bacteria and rice starch) was observed. Two forms of phagocytosis were observed for *D. fragilis* in this study which are a 'sinking' process without any apparent participation of plasma membrane extensions and the classical phagocytosis where pseudopodia were extended by amoeboid movement. The phagocytic process may occur simultaneously during the division of parasite.

By electron microscopy, *D. fragilis* usually has a spherical or oval shape, though some are amoeboid with a finely granular cytoplasm. Trophozoites with one, two or three nuclei were quite common. The nuclear structure of *D. fragilis* more closely resembles that of trichomonads (Benchimol, 2004a) rather than that of *Entamoeba* spp (Ludvík and Shipstone, 1970; Jhingan et al., 2009) or *Histomonas* spp (Zaragatzki et al., 2010). The cell division occurred by binary fission i.e. simple constriction of the cell body (Fig 3: C, D) as described before (Johnson et al., 2004). Nuclear division was found only in mononucleated trophozoites as previously reported (Wenrich, 1939; Dobell, 1940). In

some cells chromatin bodies are not prominent; perhaps such nuclei are approaching the interphase stages. Previous studies have reported the presence of microtubules in the nucleus which apparently penetrate through the nuclear membrane into the nucleoplasm forming a transnuclear spindle (Camp et al., 1974; Silard et al., 1984). These were not observed in this present study.

A prominent Golgi complex was observed in mononucleate organism in all isolates**.** In the binucleated cell the Golgi complex was mostly fragmented as reported earlier (Silard et al., 1984). It is believed that the Golgi complex in trichomonads may be involved in the processing of adhesion proteins that mediate the interaction of cells with host cells (Alderete and Garza, 1988; Arroyo et al., 1992; Shaia et al., 1998). Both smooth and rough ER were also clearly seen around the nucleus and sometimes closely associated with the hydrogenosomes, food vacuoles and microtubules.

Hydrogenosomes were observed in all four isolates and the number varied between 5-15 per trophozoite. These organelles were termed previously as "microbody-like" inclusions for *D. fragilis* (Johnson et al., 2004) and were presumed to be homologous to the paraxostylar granules of trichomonads (Camp et al., 1974). These inclusions were subsequently recognized as being hydrogenosomes (Müller, 1975). In trichomonads they are found close to the axostyle and costa (Benchimol and Souza, 1983; Benchimol, 2000). The matrix of the hydrogenosome is homogeneously granular like other trichomonads (Benchimol, 2004a).

Hydrogenosomes are an unusual organelle found in several trichomonad species and other protists living in oxygen poor or anoxic environments (Benchimol et al., 1993; Benchimol and Engelke, 2003). They do not have mitochondria nor peroxisomes

(Benchimol, 2004a; Carlton et al., 2007). The hydrogenosome contains enzymes that probably participate in the metabolism of pyruvate and is the site of formation of ATP and molecular hydrogen (Benchimol, 2009; Shiflett and Johnson, 2010; Stairs et al., 2011). The function of hydrogenosomes in *D. fragilis* are likely to be similar and related to energy production.

Basal body structures, namely the axostyle, costa and parabasal filaments were observed in *D. fragilis* by TEM. Previous phylogenetic analyses of parabasalids observed that both the mastigont and the pelta-axostyler complex were completely lost in *D. fragilis* and whose inclusion in the Parabasalia was done on the presence of hydrogenosomes (Silberman et al., 1996; Gerbod et al., 2001; Cepicka et al., 2010). The axostyle is usually seen along the longitudinal axis of the cell in trichomonads by TEM (Benchimol, 2004a). The appearance of axostyle tips as "sticking out" from the posterior end of the cell was also observed in trichomonads by SEM (Borges et al., 2004) but such arrangements for axostyle were not observed in *D. fragilis*.

No flagella was observed by SEM and TEM showing that *D. fragilis has* permanently lost its flagella. Like trichomonads (Benchimol, 2004a) and *Histomonas* (Schuster, 1968; Honigberg and Bennett, 1971) the parabasal apparatus of *D. fragilis* consists of periodic filaments that often appeared V –shaped in section (Camp et al., 1974). Clusters of parabasal apparatus were also observed in some cells in this study. Camp *et al* (1974) reported that this parabasal filament and the overlying Golgi complex correspond to the trichomonad parabasal apparatus. It was described that the polar complex is mainly a paired nonperiodic element found in dividing organism (Camp et al.,

1974). It contains microtubule structures with an affiliation with spindle microtubules. Similar observations were made in this study.

The presence of Virus-like particles are very common in other parasitic protozoa but there was no previous evidence for the existance of a VLP in *D. fragilis*. Most VLPs of protozoa are dsRNA viruses ranging in 30-200 nm in diameter and the size of their genome is 5-7 kb (Wang and Wang, 1991a, b; Benchimol et al., 2002). dsRNA viruses are also found in several isolates of *T. vaginalis* (Wang, 1985; Wang and Wang, 1986a; Benchimol, 2004a), *Giardia* (Wang and Wang, 1986b), *Leishmania* (Tarr, 1988) and *Eimeria* (Revets et al., 1989; Ellis and Revets, 1990). Kasprzak (1995) stated that all of the RNA viruses observed in parasitic protozoa showed several similarities and did not considerably differ from the viruses found in simple eukaryotic cells; they closely correspond to dsRNA viruses of yeast (Kasprzak and Majewska, 1995). It is reported that the presence of VLPs within *T. vaginalis* is associated with expression of immunogenic proteins on the trichomonad surface, variations in protozoal phenotypes, and upregulation of certain proteins, including known virulence factors and disease pathogenesis (Gerhold et al., 2009; Fraga et al., 2011; Malla et al., 2011). The identification of a VLP in *D. fragilis* in this study, for the first time, extends the distribution of VLPs to another inhabitant of the human gut.

Almost all previous studies dealing with microscopic observations of *D. fragilis* described that the characteristics of *D. fragilis* varies greatly according to the samples taken, culture conditions or fecal smears (Craig, 1926; Wenrich, 1939; Dobell, 1940; Wenrich, 1944a; Johnson et al., 2004). The present study includes a comparative analysis of nuclei number by both light and confocal microscopy of fecal smears and cultures. The

confocal microscopy showed that the cultivated trophozoite (reaching about 25 μm in size) appeared more or less spherical or showed amoeba -like morphology. Much larger sizes of trophozoite were found in cultured trophozoites compared to clinical samples. This finding supports previous observations (Silard et al., 1979). The diameter of nuclei of *D. fragilis* were from 0.5 to 3.5 μm in cultured trophozoites from all four isolates which is similar to that reported (Johnson et al., 2004). In permanently stained smears, 60% of trophozoites were binucleate whereas 70% of *in vitro* cultured trophozoites were mononucleate. This observation is also consistent with previous studies (Jepps and Dobell, 1918; Wenrich, 1944b; Windsor et al., 2003; Johnson et al., 2004; Stark et al., 2006). Dobell (1940) reported that the morphology of *D. fragilis* as seen in stools discharged from the human body differs considerably from that observable in flourishing cultures. This is partly because most specimens in faeces are not viable and so do not present a true picture of the structure of this organism (Dobell, 1940).

The cytoplasm of *D. fragilis* appears granular, vacuolated and densely filled with mainly food vacuoles containing either rice starch or bacteria and this has been observed before (Dobell, 1940; Johnson et al., 2004). In both stained smears and *in vitro* cultures, one of the granules (typically with starch) is larger than the others. Similarly, numerous food vacuoles are present in *Histomonas meleagridis* (Munsch et al., 2009). In the nucleus, the chromatin material accumulates around the periphery and the nucleolus is centrally situated. The nucleus divides non-synchronously within a cell and cell division is not always associated with synchronous replication of the DNA within these nuclei. Cell division also occurs nonsynchronously in *G. lamblia* (Kabnick and Peattie, 1990). A previous study showed that in stained smears, using iron–haematoxylin the nuclear

membrane is delicate and does not possess any peripheral chromatin (Stark et al., 2006). It is noteworthy to mention that, the structure of *D. fragilis* also varies greatly, as observed in stained preparations, with the degree of differentiation of the stain, and unless the preparations are well differentiated, the typical appearance of the karyosome is entirely lost.

An unusual feature of *D. fragilis* is the presence of two nuclei in the same trophozoite. *Dientamoeba fragilis* is not alone in this respect, since others like *Giardia* also possess two nuclei. The two nuclei of *D. fragilis* trophozoites were shown to be equivalent with respect to the amount of DNA contained in each. The approximate cell volume and nuclear volume of four isolates of *D. fragilis* were also obtained and the findings are comparable to *Trichomonas* sp. (Zubácová et al., 2008). The changes observed during cell culture of the number of nuclei present in trophozoites indicates a stage containing two nuclei is probably an intermediary of cell division.

To conclude, despite its widespread occurrence and associated symptoms, remarkably little is known about the biology and pathogenicity of *D. fragilis*. For the first time, the characteristics and ultrastructure of *D. fragilis* is described here in great detail. Three dimensional surface structures observed by SEM and ultrastructural detail observations by TEM showed that there is no significant differences between these four isolates except for possibly the presence of Virus-like-Particles (VLPs) which need further investigations. This study was only possible because of the recent major advances made in the culture of *D. fragilis* (Barratt et al., 2010).

Acknowledgements

This study was supported by funds from University of Technology, Sydney and the Australian Research Council. All electron microscopy was conducted at the Macquarie University microscopy unit. The authors thank Ms Nicole Vella for technical assistance. We also wish to express our appreciation to Dr. Michael Johnson for his support with confocal microscopy and Mr Andrew Liew for providing the image software.

References

Abraham, R., Honigberg, B.M., 1964. Structure of Trichomonas gallinae (Rivolta). J.Parasitol. 50, 608-619.

Adam, R.D., 2001. Biology of Giardia lamblia. Clin. Microbiol. Rev. 14, 447-475.

Alderete, J.F., Garza, G.E., 1988. Identification and properties of Trichomonas vaginalis proteins involved in cytadherence. Infect. Immun. 56, 28-33.

Arroyo, R., Engbring, J., Alderete, J.F., 1992. Molecular basis of host epithelial cell recognition by Trichomonas vaginalis. Mol. Microbiol. 6, 853-862.

Barratt, J.L., Banik, G.R., Harkness, J., Marriott, D., Ellis, J.T., Stark, D., 2010. Newly defined conditions for the in vitro cultivation and cryopreservation of Dientamoeba fragilis: new techniques set to fast track molecular studies on this organism. Parasitology. 137, 1867-1878.

Barratt, J.L.N, Harkness, J., Marriott, D., Ellis, J.T., Stark, D., 2011a. A review of Dientamoeba fragilis carriage in humans: Several reasons why this organism should be considered in the diagnosis of gastrointestinal illness. Gut Microbes. 2, 3-12.

Barratt, J.L., Harkness, J., Marriott, D., Ellis, J.T., Stark, D., 2011b. The ambiguous life of Dientamoeba fragilis: the need to investigate current hypotheses on transmission. Parasitology. 138, 557-572.

Benchimol, M., D Souza, W., 1983. Fine structure and cytochemistry of the hydrogenosome of Tritrichomonas foetus. J. Protozool. 30, 422-425.

Benchimol, M., Kachar, B., de Souza, W., 1993. The structural organization of the pathogenic protozoan Tritrichomonas foetus as seen in replicas of quick frozen, freeze-fractured and deep etched cells. Biol. Cell. 77, 289-295.

Benchimol, M., Almeida, J.C., de Souza, W., 1996. Further studies on the organization of the hydrogenosome in Tritrichomonas foetus. Tissue Cell. 28, 287-299.

Benchimol, M., Leal, D., Mattos, A., Diniz, J.A.P., 1997. Fine structure of Trichomonas gallinae. Biocell. 21, 47-58.

Benchimol, M., 2000. Ultrastructural characterization of the isolated hydrogenosome in Tritrichomonas foetus. Tissue Cell. 32, 518-526.

Benchimol, M., Monteiro, S., Chang, T.H., Alderete, J.F., 2002. Virus in Trichomonas--an ultrastructural study. Parasitol. Int. 51, 293-298.

Benchimol, M., Engelke, F., 2003. Hydrogenosome behavior during the cell cycle in Tritrichomonas foetus. Biol Cell. 95, 283-293.

Benchimol, M., 2004a. Trichomonads under microscopy. Microsc. Microanal. 10, 528-550.

Benchimol, M., 2004b. Mitosis in Giardia lamblia: Multiple modes of cytokinesis. Protist. 155, 33-44.

Benchimol, M., 2009. Hydrogenosomes under microscopy. Tissue Cell. 41, 151-168.

Borges, F.P., Gottardi, B., Stuepp, C., Larré, A.B., de Brum Vieira, P., Tasca, T., De Carli, G.A, 2007. Morphological aspects of Monocercomonas sp. and investigation on probable pseudocysts occurrence. Parasitol. Res. 101, 1503-1509.

Borges, F.P., Wiltuschnig, R.C., Tasca, T., De Carli, G.A., 2004. Scanning electron microscopy study of Tritrichomonas augusta. Parasitol Res. 94, 158-161.

Camp, R.R., Mattern, C.F., Honigberg, B.M., 1974. Study of Dientamoeba fragilis Jepps & Dobell. I. Electronmicroscopic observations of the binucleate stages. II. Taxonomic position and revision of the genus. J. Protozool. 21, 69-82.

Carlton, J.M., Hirt, R.P., Silva, J.C., Delcher, A.L., Schatz, M., Zhao, Q., Wortman, J.R., Bidwell, S.L., Alsmark, U.C.M., Besteiro, S.b., Sicheritz-Ponten, T., Noel, C.J., Dacks, J.B., Foster, P.G., Simillion, C., Van de Peer, Y., Miranda-Saavedra, D., Barton, G.J., Westrop, G.D., Müller, S, Dessi, D., Fiori, P.L., Ren, Q., Paulsen, I., Zhang, H., Bastida-Corcuera, F.D., Simoes-Barbosa, A., Brown, M.T., Hayes, R.D., Mukherjee, M., Okumura, C.Y., Schneider, R., Smith, A.J., Vanacova, S., Villalvazo, M., Haas, B.J., Pertea, M., Feldblyum, T.V., Utterback, T.R., Shu, C.-L., Osoegawa, K., de Jong, P.J., Hrdy, I., Horvathova, L., Zubacova, Z., Dolezal, P., Malik, S.-B., Logsdon, J.M., Henze, K., Gupta, A., Wang, C.C., Dunne, R.L., Upcroft, J.A., Upcroft, P., White, O., Salzberg, S.L., Tang, P., Chiu, C.-H., Lee, Y.-S., Embley, T.M., Coombs, G.H., Mottram, J.C., Tachezy, J., Fraser-Liggett, C.M., Johnson, P.J., 2007. Draft genome sequence of the sexually transmitted pathogen Trichomonas vaginalis. Science 315, 207-212.

Cepicka, I., Hampl, V., Kulda, J., 2010. Critical taxonomic revision of Parabasalids with description of one new genus and three new species. Protist. 161, 400-433.

Cerva, L., Nohýnková, E., 1992. A light microscopic study of the course of cellular division of Giardia intestinalis trophozoites grown in vitro. Folia. Parasitol. 39, 97-104.

Chen, W., Chen, J., Zhong, X., Lin, X., Chen, L., 2004. [Electron microscopic study on Trichomonas vaginalis adhering to and phagocytizing male genitourinary epithelial cells]. Zhonghua Nan Ke Xue. 10, 86-89.

Craig, C.F., 1926. The nuclear structure of Dientamoeba fragilis. J. Parasitol. 13, 137-140.

Delgado-Viscogliosi, P., Viscogliosi, E., Gerbod, D., Kulda, J., Sogin, M.L., Edgcomb, V.P., 2000. Molecular phylogeny of parabasalids based on small subunit rRNA sequences, with emphasis on the Trichomonadinae subfamily. J. Eukaryot. Microbiol. 47, 70-75.

Dobell, C., 1940. Researches on the intestinal protozoa of monkeys and man. X. The life history of Dientamoeba fragilis: observations, experiments and speculations. Parasitology. 32, 417-461.

Ellis, J., Revets, H., 1990. Eimeria species which infect the chicken contain virus-like RNA molecules. Parasitology. 101, 163-169.

Fraga, J., Rojas, L., Sariego, I., Fernández-Calienes, A., 2011. Double-stranded RNA viral infection of Trichomonas vaginalis and correlation with genetic polymorphism of isolates. Exp Parasitol. 127, 593-599.

Gerbod, D., Edgcomb, V.P., Noël, C., Zenner, L., Wintjens, R., Delgado-Viscogliosi, P., Holder, M.E., Sogin, M.L., Viscogliosi, E., 2001. Phylogenetic position of the trichomonad parasite of turkeys, Histomonas meleagridis (Smith) Tyzzer, inferred from small subunit rRNA sequence. J. Eukaryot. Microbiol. 48, 498-504.

Gerbod, D., Noël, C., Dolan, M.F., Edgcomb, V.P., Kitade, O., Noda, S., Dufernez, F., Ohkuma, M., Kudo, T., Capron, M., Sogin, M.L., Viscogliosi, E., 2002.

Molecular phylogeny of parabasalids inferred from small subunit rRNA sequences, with emphasis on the Devescovinidae and Calonymphidae (Trichomonadea). Mol. Phylogenet. Evol. 25, 545-556.

Gerhold, R.W, Allison, A.B, Sellers, H., Linnemann, E., Chang, T.H., Alderete, J.F, 2009. Examination for double-stranded RNA viruses in Trichomonas gallinae and identification of a novel sequence of a Trichomonas vaginalis virus. Parasitol. Res. 105, 775-779.

Granger, B.L., Warwood, S.J., Benchimol, M., De Souza, W., 2000. Transient invagination of flagella by Tritrichomonas foetus. Parasitol Res. 86, 699-709.

Honigberg, B.M., Bennett, C.J., 1971. Lightmicroscopic observations on structure and division of Histomonas meleagridis (Smith). J Protozool. 18, 687-697.

Honigberg, B.M., Daniel, W.A., Mattern, C.F., 1972. Fine Structure of Trichomitus batrachorum (Perty). J Protozool. 19, 446-453.

Honigberg, B.M., 1978. Trichomonads of veterinary importance. In: Kreier, J.P. (Ed.), Parasitic Protozoa, Academic Press. New York, 163-273.

Jahn, C.L., Klobutcher, L.A., 2002. Genome remodeling in ciliated protozoa. Annu Rev Microbiol. 56, 489-520.

Jepps, M.W., Dobell, C., 1918. Dientamoeba fragilis n.g., n. sp., new intestinal amoeba from man. Parasitology. 10, 352-367.

Jhingan, G.D., Panigrahi, S.K., Bhattacharya, A., Bhattacharya, S., 2009. The nucleolus in Entamoeba histolytica and Entamoeba invadens is located at the nuclear periphery. Mol Biochem Parasitol. 167, 72-80.

Johnson, E.H., Windsor, J.J., Clark, C.G., 2004. Emerging from obscurity: biological, clinical, and diagnostic aspects of Dientamoeba fragilis. Clin Microbiol Rev. 17, 553-570.

Kabnick, K.S., Peattie, D.A., 1990. In situ analyses reveal that the two nuclei of Giardia lamblia are equivalent. J Cell Sci. 95, 353-360.

Kasprzak, W., Majewska, A.C., 1995. [Viruses of parasitic protozoa]. Wiad Parazytol. 41, 131-137.

Kietzmann GE, J.r., 1993. Relationships of Trichomonas gallinae to the palatal-esophageal junction of ring doves (Streptopelia risoria) as revealed by scanning electron microscopy. J. Parasitol. 79, 408-415.

Kurnatowska, A., Hajdukiewicz, G., 1977. Trichomonas vaginalis variability in axenic cultures evaluated in scanning electron microscope. Wiad. Parazytol 23, 481-487.

Ludvík, J., Shipstone, A.C., 1970. The ultrastructure of Entamoeba histolytica. Bull World Health Organ. 43, 301-308.

Malla, N., Kaul, P., Sehgal, R., Gupta, I., 2011. The presence of dsRNA virus in Trichomonas vaginalis isolates from symptomatic and asymptomatic Indian women and its correlation with in vitro metronidazole sensitivity. Indian J Med Microbiol. 29, 152-157.

Mattern, C.F., Honigberg, B.M., Daniel, W.A., 1967. The mastigont system of Trichomonas gallinae (Rivolta) as revealed by electron microscopy. J. Protozool. 14, 320-339.

Mehlhorn, H., Al-Quraishy, S., Aziza, A., Hess, M., 2009. Fine structure of the bird parasites Trichomonas gallinae andTetratrichomonas gallinarum from cultures. Parasitol Res. 105, 751-756.

Mielewczik, M., Mehlhorn, H., Al-Quraishy, S., Grabensteiner, E., Hess, M., 2008. Transmission electron microscopic studies of stages of Histomonas meleagridis from clonal cultures. Parasitol Res. 103, 745-750.

Moody, A.H., Fleck., S.L., 1985. Versatile Field's stain. J. Clin. Pathol. 38, 842-843.

Müller, M., 1975. Biochemistry of protozoan microbodies: peroxisomes, alpha-glycerophosphate oxidase bodies, hydrogenosomes Annu. Rev. Microbiol. 29, 467-483.

Munsch, M., Lotfi, A., Hafez, H.M., Al-Quraishy, S., Mehlhorn, H., 2009. Light and transmission electron microscopic studies on trophozoites and cyst-like stages of Histomonas meleagridis from cultures. Parasitol Res. 104, 683-689.

Ockert, G., Schneider, W., 1974. [Electron microscopic findings in Dientamoeba fragilis]. Z Gesamte Hyg 20, 555-557.

Ohkuma, M., Iida, T., Ohtoko, K., Yuzawa, H., Noda, S., Viscogliosi, E., Kudo, T., 2005. Molecular phylogeny of parabasalids inferred from small subunit rRNA sequences, with emphasis on the Hypermastigea. Mol Phylogenet Evol. 35, 646-655.

Ovcinnikov, N.M., Delektorskij, V.V., Turanova, E.N., Yashkova, G.N., 1975. Further studies of Trichomonas Vaginalis with transmission and scanning electron microscopy. Br J Vener Dis. 51, 357-375.

Prescott, D.M., 1994. The DNA of ciliated protozoa. Microbio Rev. 58, 233-267.

Revets, H., Dekegel, D., Deleersnijder, W., De Jonckheere, J., Peeters, J., Leysen, E., Hamers, R., 1989. Identification of virus-like particles in Eimeria stiedae. Mol Biochem Parasitol. 36, 209-215.

Sawangjaroen, N., Luke, R., Prociv, P., 1993. Diagnosis by faecal culture of Dientamoeba fragilis infections in Australian patients with diarrhoea. Trans R Soc Trop Med Hyg. 87, 163-165.

Schuster, F.L., 1968. Ultrastructure of Histomonas meleagridis (Smith) Tyzzer, a Parasitic Amebo-Flagellate . J. Parasitol. 54, 725-737.

Shaia, C.I., Voyich, J., Gillis, S.J., Singh, B.N., Burgess, D.E., 1998. Purification and expression of the Tf190 adhesin in Tritrichomonas foetus. Infect. Immun. 66, 1100-1105.

Shiflett, A.M., Johnson, P.J., 2010. Mitochondrion-related organelles in eukaryotic protists. Annu Rev Microbiol. 64, 409-429.

Silard, R., Colea, A., Panaitescu, D., Florescu, P., Roman, N., 1979. Studies on Dientamoeba fragilis in Romania. I. Dientamoeba fragilis isolated from clinical cases. Problems of diagnosis, incidence, clinical aspects. Arch Roum Pathol Exp Microbiol. 38, 359-372.

Silard, R., Burghelea, B., Panaitescu, D., Burcos, V., 1984. Ultrastructure of Dientamoeba fragilis: a study of the mononucleated stage. Arch Roum Pathol Exp Microbiol. 43, 87-101.

Silard, R., Burghelea, B., 1986. Endosymbionts in Dientamoeba fragilis trophozoites resistant to antiprotozoal drugs. Arch Roum Pathol Exp Microbiol. 45, 65-74.

Silberman, J.D., Clark, C.G., Sogin, M.L., 1996. Dientamoeba fragilis shares a recent common evolutionary history with the trichomonads. Mol Biochem Parasitol 76, 311-314.

Southern, E.M., 1975. Detection of specific sequences among DNA fragments separated by gel electrophoresis. J. Mol. Biol. 98, 503-517.

Stabler, R.M., 1941. The morphology of Trichomonas gallinae (= columbae). J Morphol. 69, 501-515.

Stabler, R.M., 1954. Trichomonas gallinae: a review. Exp Parasitol. 3, 368-402.

Stairs, C.W., Roger, A.J., Hampl, V., 2011. Eukaryotic pyruvate formate lyase and its activating enzyme were acquired laterally from a firmicute. Mol Biol Evol. 28. 2087-2099.

Stark, D., Phillips, O., Peckett, D., Munro, U., Marriott, D., Harkness, J., Ellis, J., 2008. Gorillas are a host for Dientamoeba fragilis: an update on the life cycle and host distribution. Vet Parasitol. 151, 21-26.

Stark, D., Barrat, J., Roberts, T., Marriot, D., Harkness, J., Ellis, J., 2010a. Comparison of microscopy, two xenic culture techniques, conventional and real-time PCR for the detection of Dientamoeba fragilis in clinical stool samples. Eur J Clin Microbiol Infect Dis. 29, 411-416.

Stark, D., Barratt, J., Roberts, T., Marriott, D., Harkness, J., Ellis, J., 2010b. A review of the clinical presentation of dientamoebiasis. Am J Trop Med Hyg. 82, 614-619.

Stark, D.J., Beebe, N., Marriott, D., Ellis, J.T., Harkness, J., 2006. Dientamoebiasis: clinical importance and recent advances. Trends Parasitol. 22, 92-96.

Svärd, S.G., Hagblom, P., Palm, J.E., 2003. Giardia lamblia -- a model organism for eukaryotic cell differentiation. FEMS Microbiol Lett 218, 3-7.

Tarr, P.I., Aline, RF, J.r., Smiley, B.L. , Scholler, J., Keithly, J., Stuart, K . 1988. LR1: a candidate RNA virus of Leishmania. Proc Natl Acad Sci U S A. 85, 9572-9575.

Tasca, T., De Carli, G.A., 2003. Scanning electron microscopy study of Trichomonas gallinae. Vet Parasitol. 118, 37-42.

Tasca, T., De Carli, G.A., 2007. Morphological study of Tetratrichomonas didelphidis isolated from opossum Lutreolina crassicaudata by scanning electron microscopy. Parasitol Res 100, 1385-1388.

Wang, A.L., Wang, C.C., 1986a. The double-stranded RNA in Trichomonas vaginalis may originate from virus-like particles. Proc Natl Acad Sci U S A. 83, 7956-7960.

Wang, A.L., Wang, C.C., 1986b. Discovery of a specific double-stranded RNA virus in Giardia lamblia. Mol Biochem Parasitol. 21, 269-276.

Wang, A.L., Wang, C.C., 1991a. Viruses of the protozoa. Annu Rev Microbiol. 45, 251-263.

Wang, A.L., Wang, C.C., 1991b. Viruses of parasitic protozoa. Parasitol Today. 7, 76-80.

Wang, A.L., Wang, C. C., 1985. A linear double-stranded RNA in Trichomonas vaginalis. J Biol Chem. 260, 3697-3702.

Warton, A., Honigberg, B.M., 1979. Structure of trichomonads as revealed by scanning electron microscopy. J Protozool. 26, 56-62.

Wenrich, D.H., 1939. Studies on Dientamoeba fragilis (protozoa). III. Binary fission with special reference to nuclear division. J. Parasitol. 25, 43-45.

Wenrich, D.H., 1944a. Nuclear structure and nuclear division in Dientamoeba fragilis (Protozoa). J Morphol. 74, 467-491.

Wenrich, D.H., 1944b. Studies on Dientamoeba fragilis (protozoa). IV. Further observations, with an outline of present-day knowledge of this species. J. Parasitol. 30, 322-337.

Wiesehahn, G.P., Jarroll, E.L., Lindmark, D.G., Meyer, E.A., Hallick, L.M., 1984. Giardia lamblia: autoradiographic analysis of nuclear replication. Exp Parasitol. 58, 94-100.

Windsor, J.J., Johnson, E.H., 1999. Dientamoeba fragilis: the unflagellated human flagellate. Br J Biomed Sci 56, 293-306.

Windsor, J.J., Macfarlane, L., Hughes-Thapa, G., Jones, S.K., Whiteside, T.M., 2003. Detection of Dientamoeba fragilis by culture. Br J Biomed Sci. 60, 79-83.

Zaragatzki, E., Hess, M., Grabensteiner, E., Abdel-Ghaffar, F., Al-Rasheid, K.A., Mehlhorn, H., 2010. Light and transmission electron microscopic studies on the encystation of Histomonas meleagridis. Parasitol Res. 106, 977-983.

Zubácová, Z., Cimburek, Z., Tachezy, J., 2008. Comparative analysis of trichomonad genome sizes and karyotypes. Mol Biochem Parasitol. 161, 49-54.

Legends to figures and tables

Fig. 1. SEM showing the external surface structures of four isolates of *Dientamoeba fragilis* (I) (A) Isolate 1 (B) Isolate 2 (C) Isolate 3 (D) Isolate 4. (II) Two different populations of *Dientamoeba fragilis* exist (E) smooth cell (F) ruffled cell.

Fig. 2. SEM showing two forms of phagocytosis of *Dientamoeba fragilis*. Formation of phagocytic cup (arrow) and moving to food particles without extension of plasma membrane *(*A & B) and attachment of bacteria to the parasite occurs via the whole cell surface with pseudopodia which engulf bacteria (C & D). (B= bacteria, Rs= rice starch).

Fig. 3. SEM showing the different stages of *Dientamoeba fragilis* in culture at different time intervals. (A, B) Cells at early stages of culture (6h- 12h) showing phagocytosis and engulfing rice starch (Rs) and bacteria (B); (C, D) trophozoites are dividing by binary fission, the arrow indicates it can stretch like a bridge; (E , F) at 48 h and 72 h of cultures cells are rounded.

Fig. 4. Electron micrograph (TEM) showing the fine ultrastructure of *Dientamoeba fragilis* trophozoite (A) mononucleate (B) binucleate (C) anucleate (D) amoeboid - like with pseudopodia. (B= bacteria, Ch= chromatin bodies, Dv= digestve vacuole, G= glycogen, H= hydrogenosomes, L= lysosome, My = myelin sheath, N= nucleus, Pf= parabasal filament, Ps= pseudopodia, Rs= rice starch).

Fig. 5. (A) Nucleus structure. Nm= nuclear membrane, Ch= chromatin bodies, Np= nuclear pore (arrow) (B) formation of extranuclear spindle (arrow) during nuclear division (C) indicates binary fission (D) (Nu= nucleolus) nucleolus dividing.

Fig. 6. Organelles of *Dientamoeba fragilis* trophozoite (A) Golgi complex (B) Smooth endoplasmic reticulum (ER) (C) rough ER attaching ribosomes on it surfaces (D) Hydrogenosomes in cytoplasm (E) double layered membrane bound electron dense hydrogenosome at higher magnification (F) lysosome located near to cell membrane. (Dv= digestve vacuole, L= lysosome, Gc= golgi complex, N= nucleus, r = ribosome, m= cell membrane, H= hydrogenosome, ED= electron dense materials).

Fig. 7. Digestive vacuole of *Dientamoeba fragilis* trophozoite (A) presence of digestive vacuoles (Dv) (B) containing rod-shaped bacterium (B) and myelin sheath (My) in digestive vacuole (C) Phagocytosis (arrow) of *D. fragilis*, engulfing bacteria (D) formation of phagosome (Ph) (E) is engulfing rice starch (F) exocytosis phenomena (arrow). (B= bacteria, c= cytoplasm, Rs= Rice starch, Pm= plasmalemma).

Fig. 8. Basal body structures of *Dientamoeba fragilis* (A**)** multiple ribbons of microtubules forming the axostyle (arrow), which runs from the basal bodies to the cell tip (B) closer view of attractophore (V- shaped structure) and axostyle (Ax) (C) basal body (BB) structures (D) Costa (Co) structure in the cytoplasm (E) presence of parabasal filament (Pf) in close proximity to the nucleus (F) double layerd *D. fragilis* cell membrane (m) (c= cytoplasm, ED= electron dense materials, Mt= microtubules).

Fig. 9. TEM showing the presence of Virus-Like Particles (VLPs) in the perinuclear region (arrow) of *Dientamoeba fragilis* trophozoite. VLP is budding through the Golgi complex. (N= nucleus, Gc= Golgi complex).

Fig. 10. Iron–haematoxylin stained smears of *Dientamoeba fragilis* trophozoite (clinical samples). (A) mononucleate (B) binucleate (C) three nuclei (D) anucleate. Images were taken by Olympus DP70 at magnification 100x DiC. The scale bar is 10 μm, (N= nucleus).

Fig. 11. Morphology of DAPI stained nuclei of *Dientamoeba fragilis* trophozoite (Isolate 1). Digestive vacuoles contain either rice starch (Rs) or bacteria. (i, ii, iii) Phase image of binucleate cell (iv, v, vi) mononucleate cell (vii, viii, ix) anucleate cell. Magnification, 100X DiC. The scale bar is 5 μm, (N= nucleus).

Fig. 12. Comparison of numbers of nuclei in *Dientamoeba fragilis* trophozoites at different time intervals during *in vitro* culture (Isolate 1).

Fig. 13. Nile Red staining *Dientamoeba fragilis* trophozoite and DAPI stained nuclei showing the cell volume. (A) Nile Red stained mononucleate (B) binucleate (C) anucleate (D) *D. fragilis* exhibiting phagocytosis found form cultured condition. Magnification, 100X DiC. The scale bar is 3 μm. (Rs= rice starch and N= Nucleus).

Table 1

Comparison of DNA content of nuclei from four *Dientamoeba fragilis* isolates (total cell number was 100, 25 binucleate cells from each isolate). Only trophozoites containing two nuclei were used.

Table 2

Comparison of cell dimensions and approximate volumes of four isolates of *Dientamoeba fragilis* (total cell number was 200; 50 non-dividing cells from each isolate).

Table 3

Ultrastructural characteristics of the organelles of *Dientamoeba fragilis*.

Table 1

D. fragilis isolates	Left nucleus §	Right nucleus §	§Left-Right*	t-stat/d.f*	P value
Isolate 1	1.95	1.93	0.02±0.09	0.349/48	0.72 (NS)
Isolate 2	1.19	1.17	0.02± 0.06	0.254/48	0.79 (NS)
Isolate 3	1.62	1.49	0.13±0.05	0.985/48	0.32 (NS)
Isolate 4	1.47	1.45	0.02±0.02	0.242/48	0.80 (NS)

§ Average of arbitrary units of fluorescence of 25 determinations of each isolate; cellular background fluorescence has been subtracted.

* t-stat/ degree of freedom

Table 2

D. fragilis isolates	Cell dimensions		Cell volume V*=3/4 πab^2 (µm^3)	Nucleus dimensions		Nucleus volume V*=3/4 πab^2 (µm^3)
	Length$^+$ (µm) mean±SD	Width$^+$ (µm) mean±SD		Length$^+$ (µm) mean±SD	Width$^+$ (µm) mean±SD	
Isolate 1	11.91±2.33	6.00±1.25	1.0	1.8±0.52	0.97±0.33	0.003
Isolate 2	11.78±2.79	5.88±1.39	0.9	2.28±0.74	1.12±0.32	0.006
Isolate 3	12.07±2.93	6.01±1.45	1.0	1.50±0.38	0.73±0.22	0.001
Isolate 4	12.69±3.99	7.40±3.03	1.6	2.09±0.61	1.11±0.49	0.006

$^+$Average of 50 trophozoites±standard deviation

* The cell volume was calculated according to the formula V=3/4πab^2; "*a*" is the cell length; "*b*" is the cell width. (π = 3.14)

Table 3

Name	Characteristics	Sizes
Nucleus	One , two or three; mostly spherical; located in the central region of cell; double membrane containing numerous nuclear pores; usually containing two to eight chromatin bodies without peripheral chromatin	0.86-3.52 μm
Golgi complex	Vesicular structure generally located in the perinuclear area; 7-10 cisternae	About 450 nm long
Endoplasmic reticulum	Smooth and rough endoplasmic reticulums were observed; found around the nucleus	About 500 nm long
Hydrogenosomes	Spherical or oval shaped ; double layered membrane; located in the cytoplasm; 5 to 15 per cell	0.12-0.83μm
Digestive vacuoles	Found throughout the cytoplasm; 1-10 per cell	0.59- 4.2 μm
Lysosomes	Located mainly in the posterior region of the cell in close proximity to the cell membrane	0.50- 2 μm
Basal body components		
Axostyle	Microtubular ribbon; usually found in the anterior region of the cell	
Costa	Proteinaceous structure	
Parabasal filament	Located near to nucleus; singular or in a cluster form; formed by 30 to 40 hairy –like segments	

Figure 1
Click here to download high resolution image

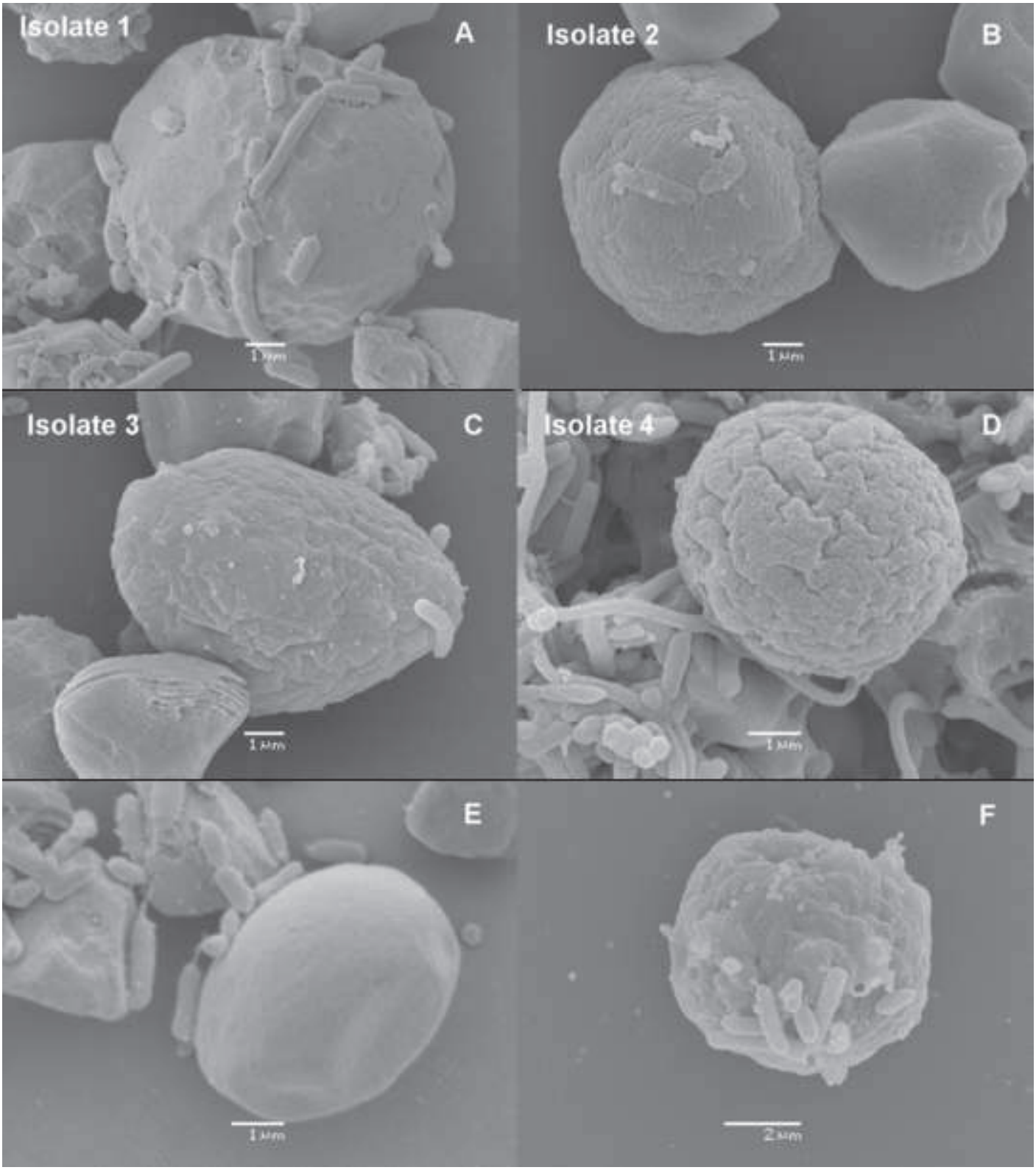

Figure 2

Click here to download high resolution image

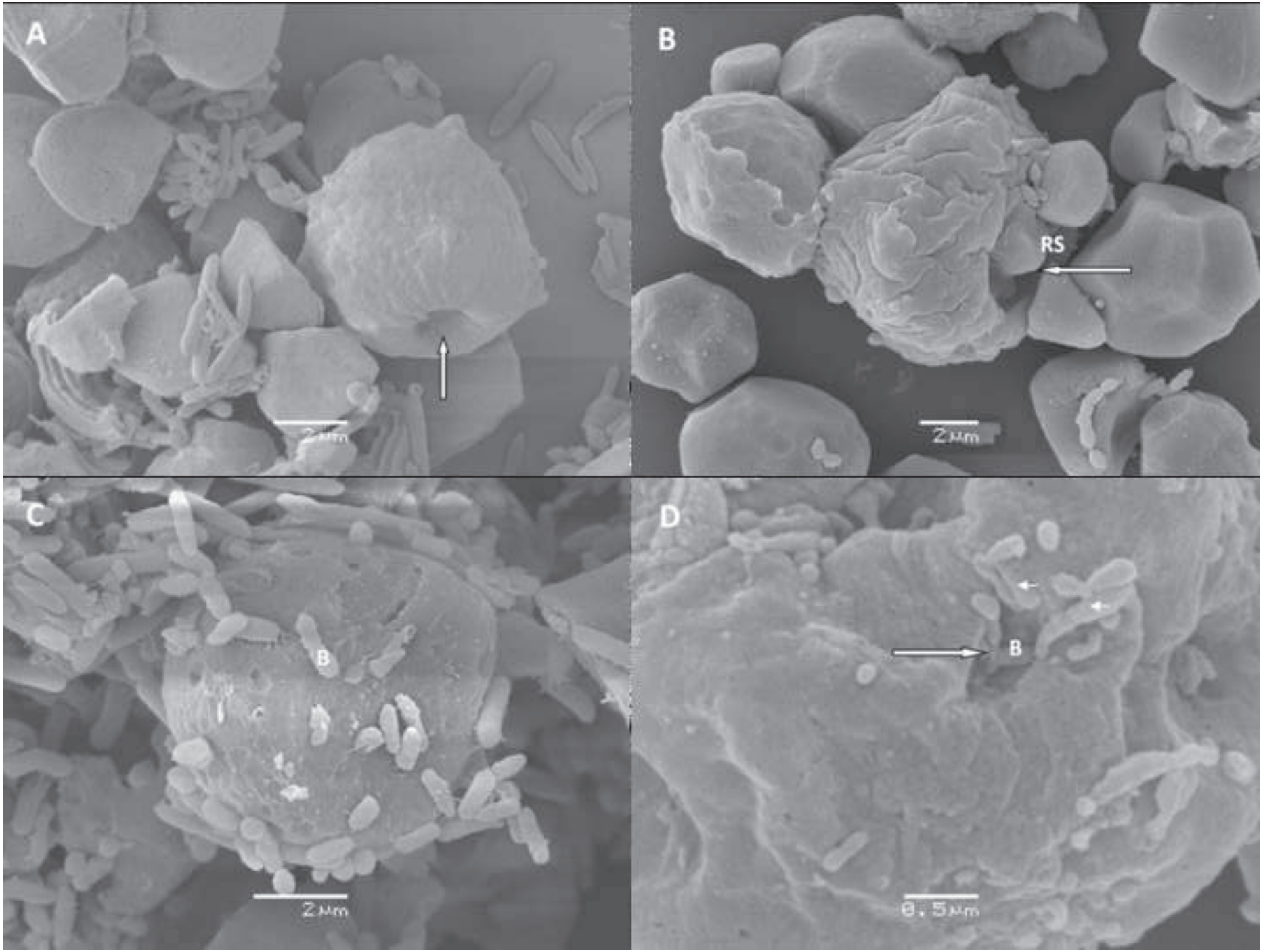

Figure 3
Click here to download high resolution image

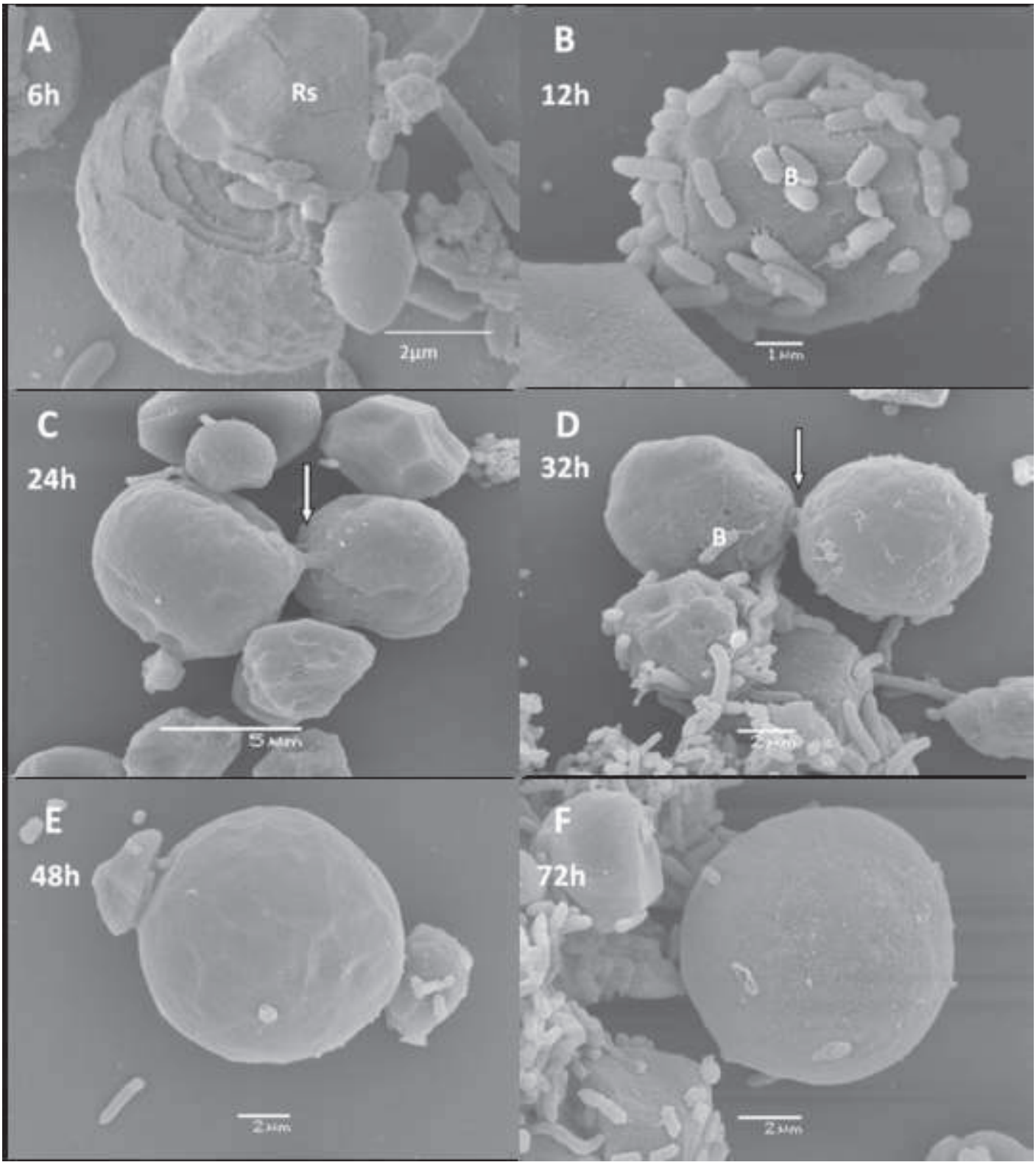

Figure 4

Click here to download high resolution image

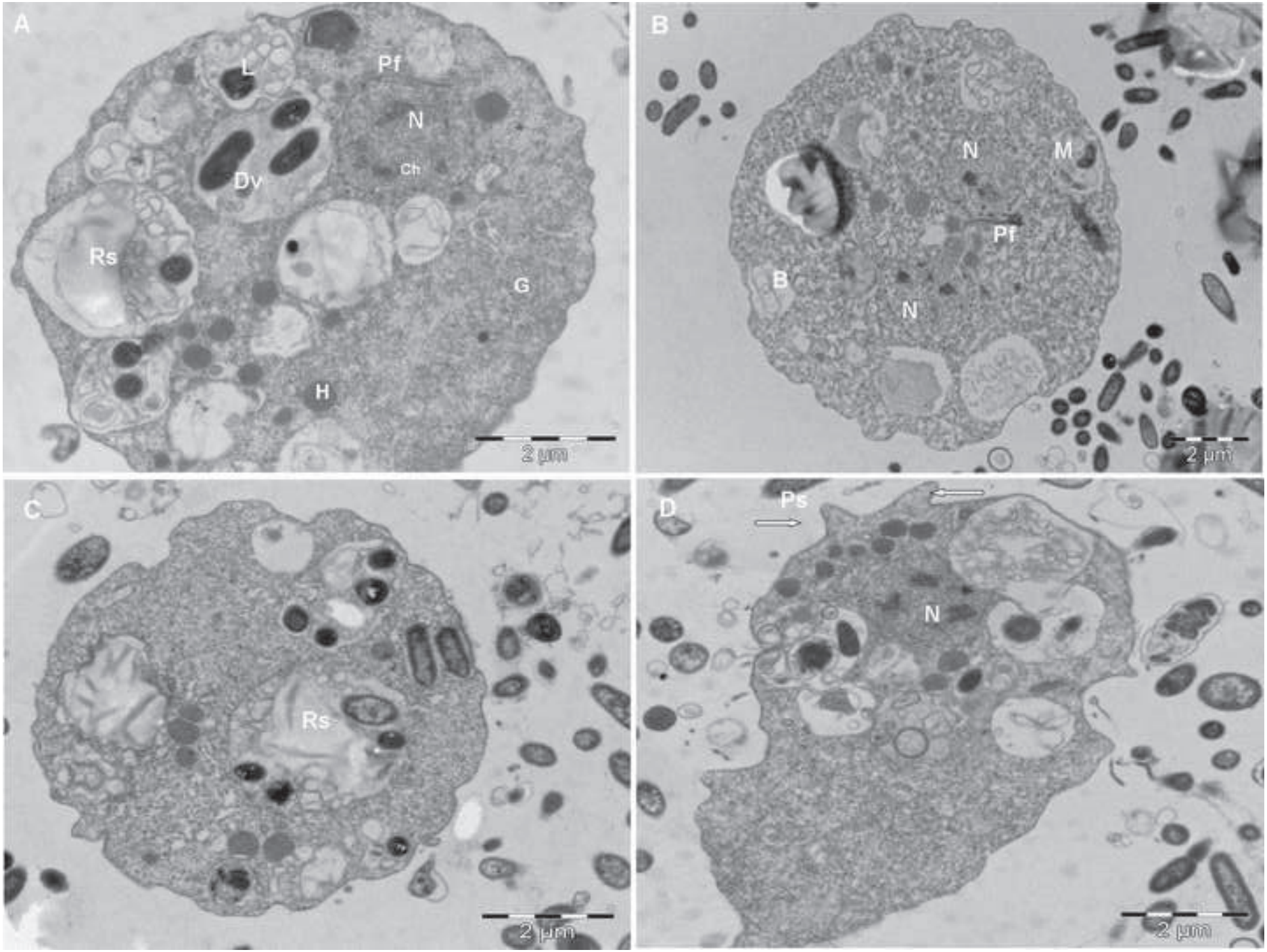

Figure 5

Click here to download high resolution image

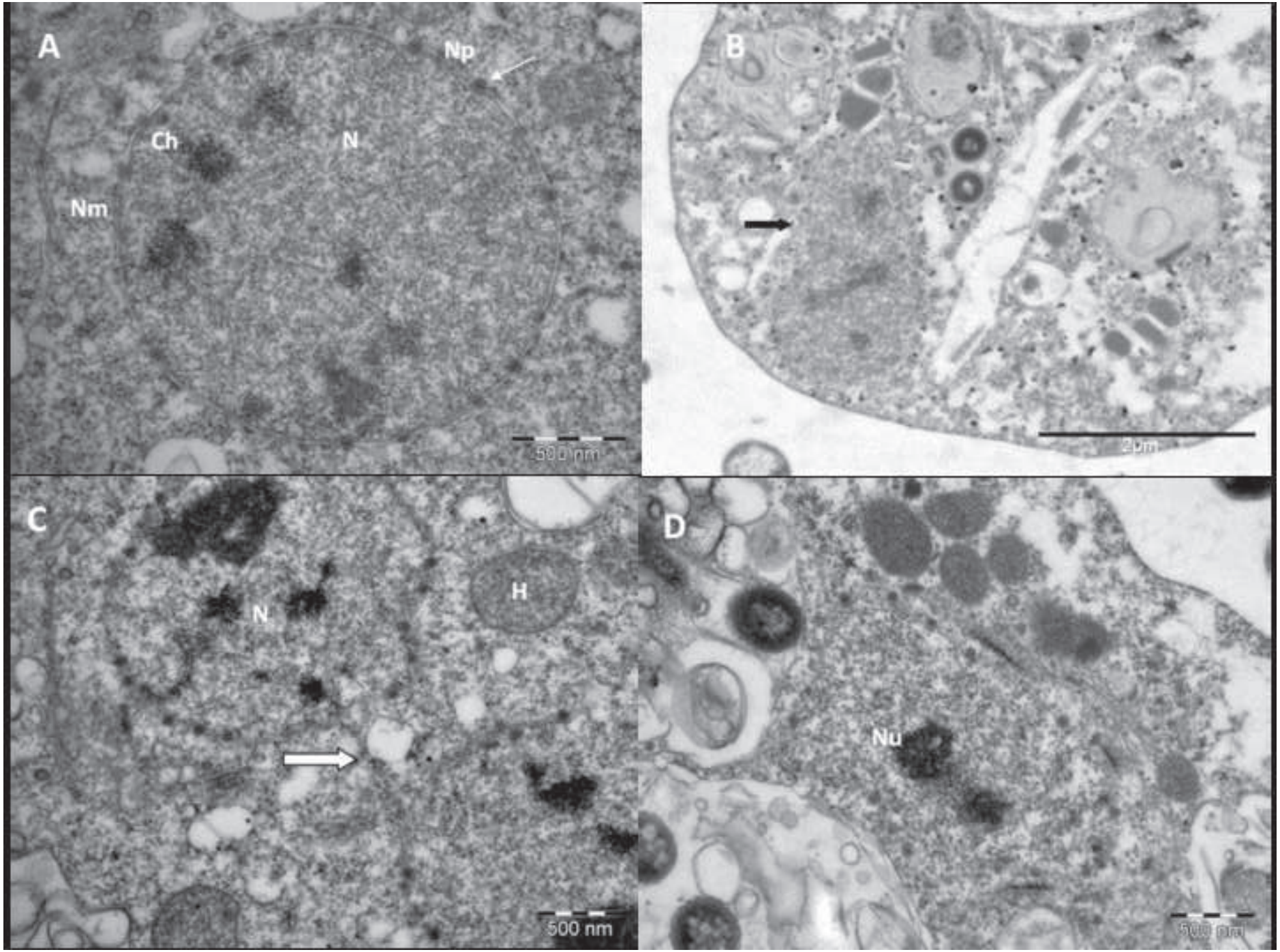

Figure 6

Click here to download high resolution image

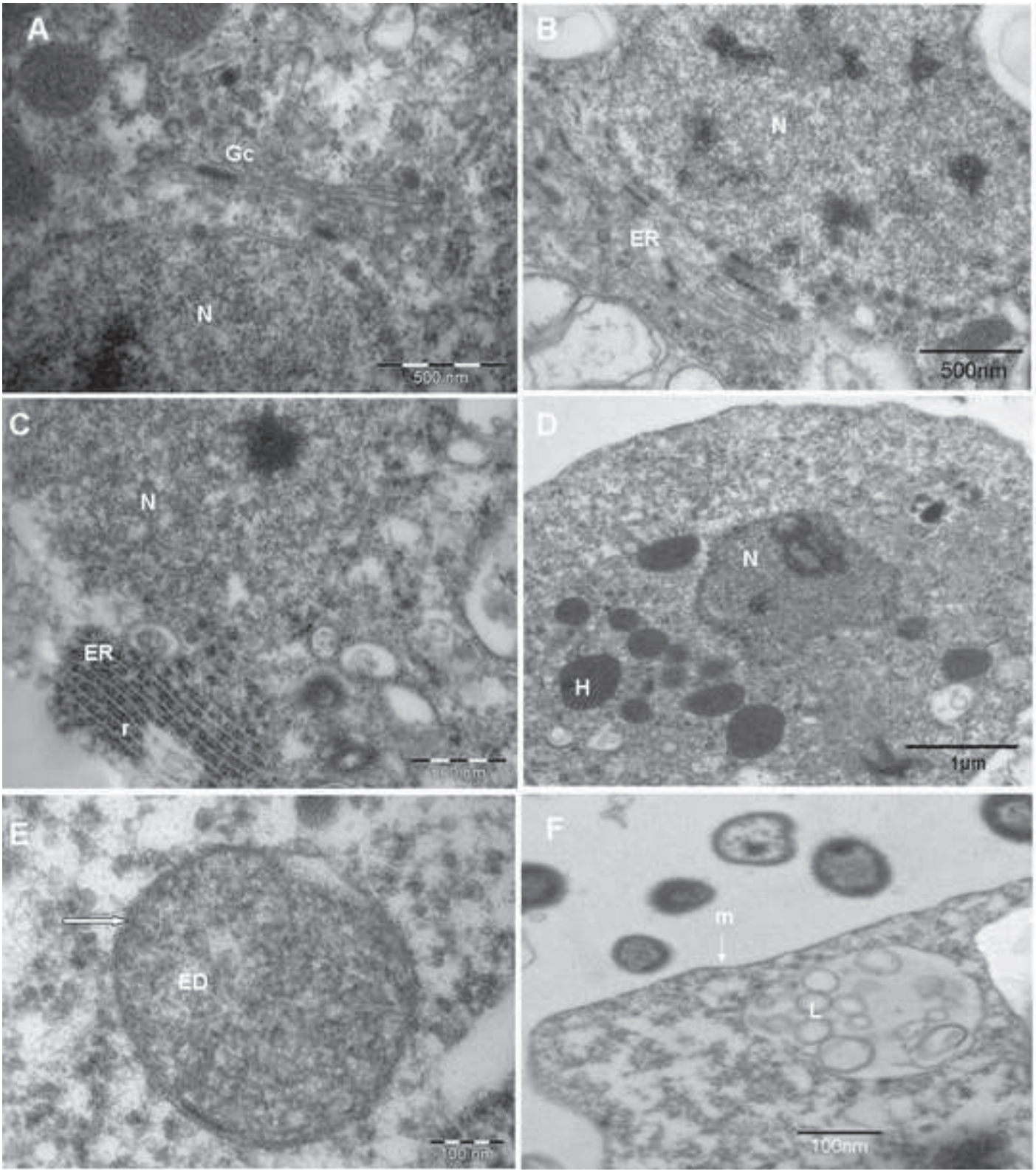

Figure 7
Click here to download high resolution image

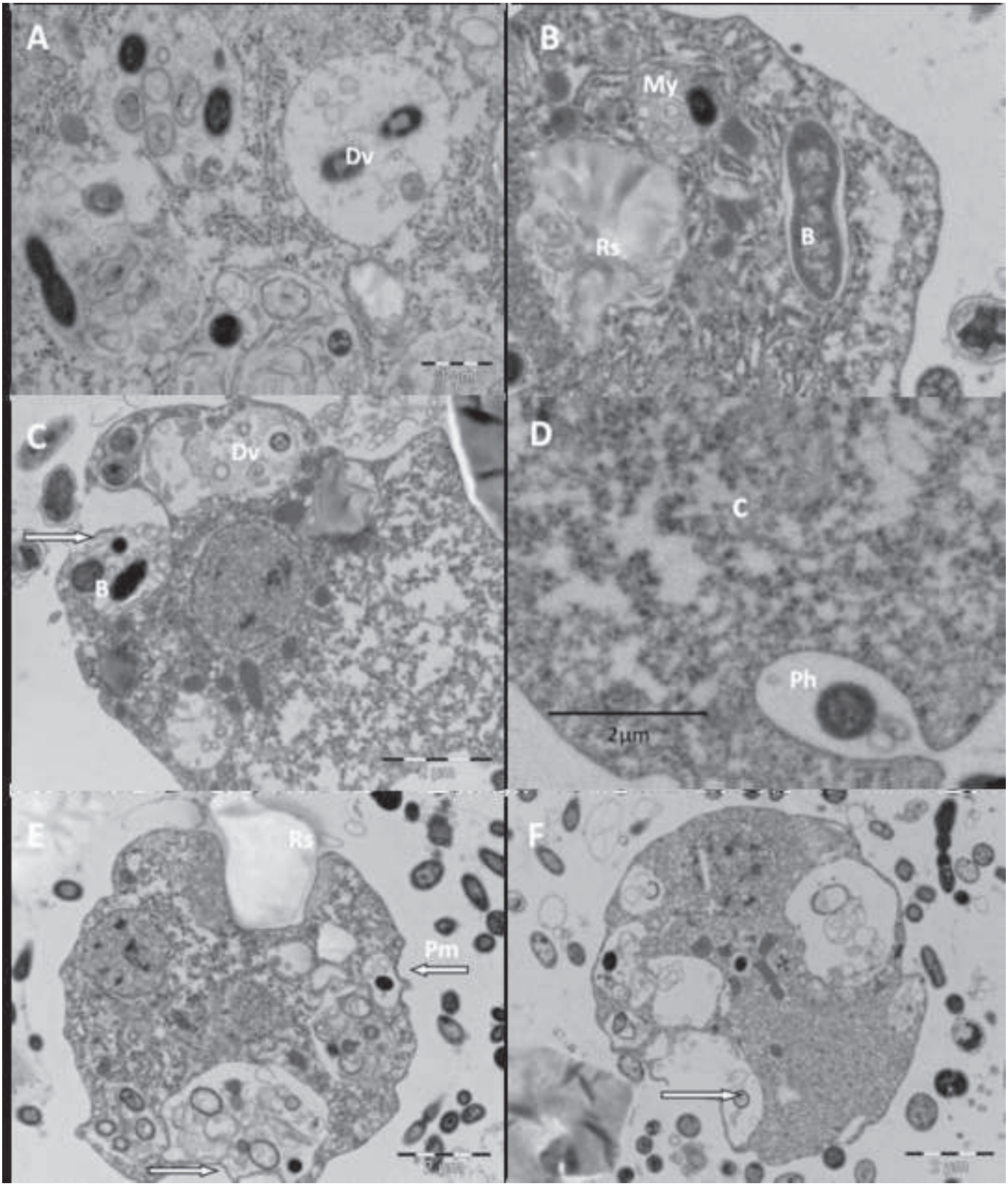

Figure 8
Click here to download high resolution image

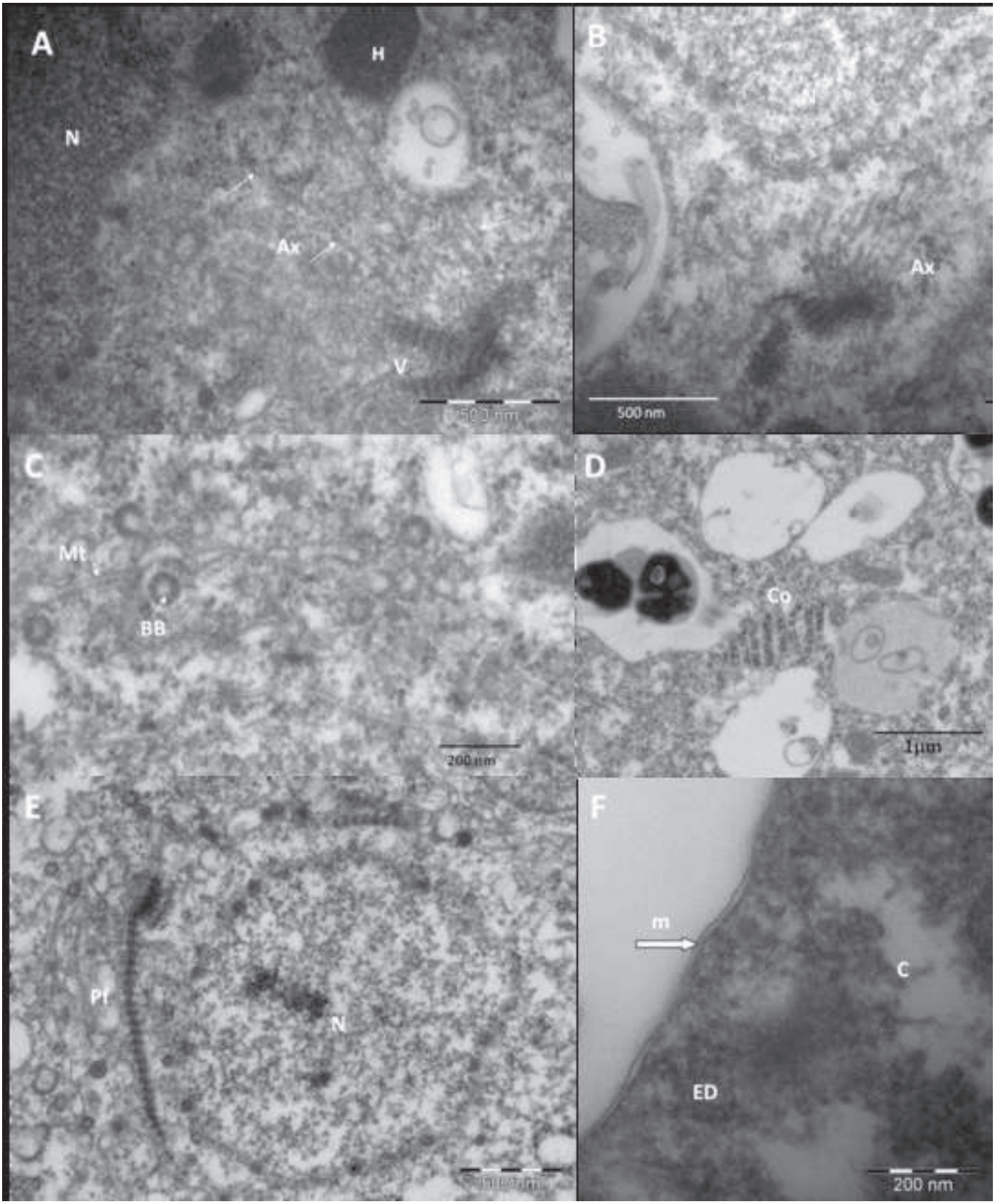

Figure 9

Click here to download high resolution image

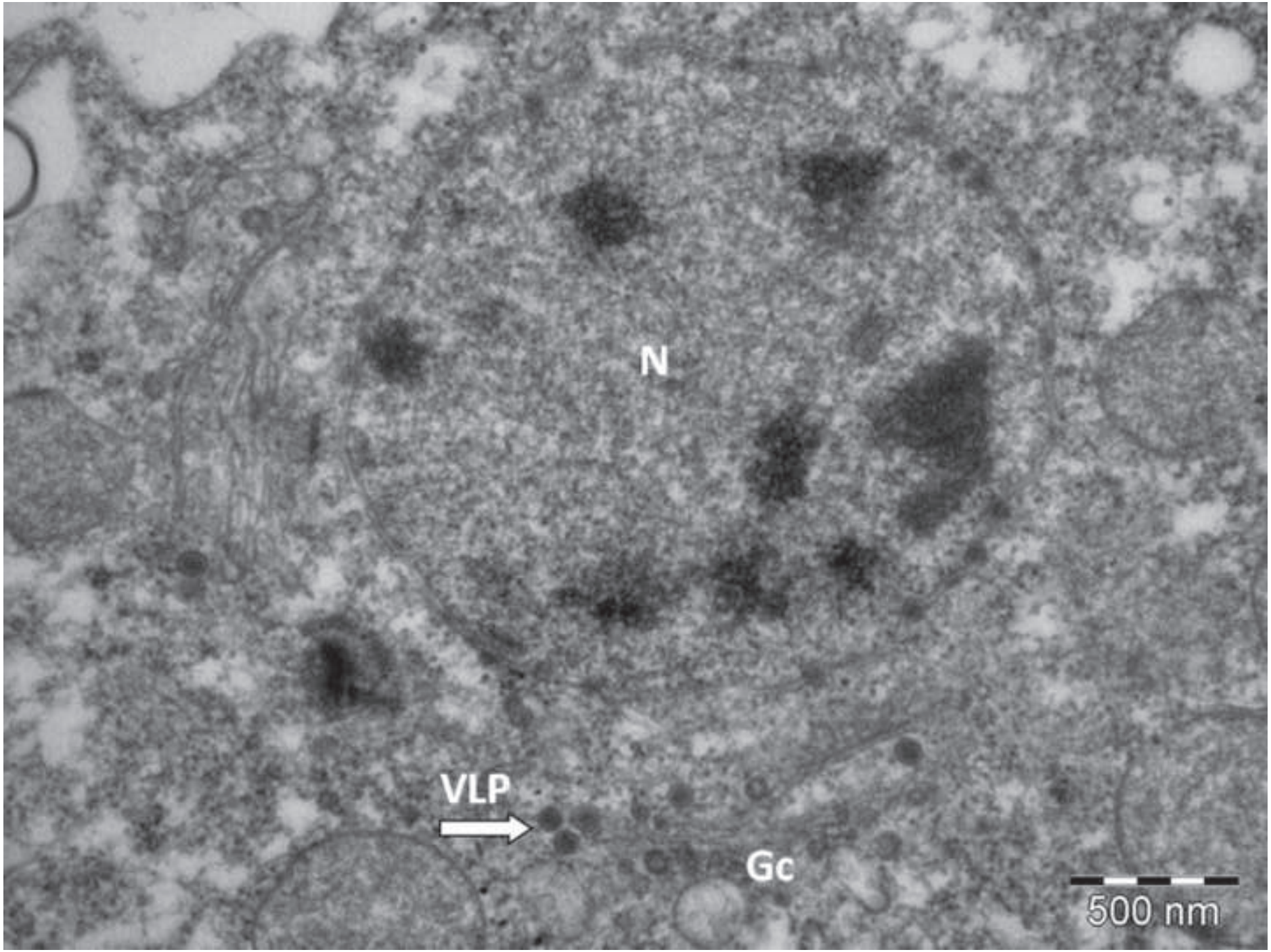

Figure 10

Click here to download high resolution image

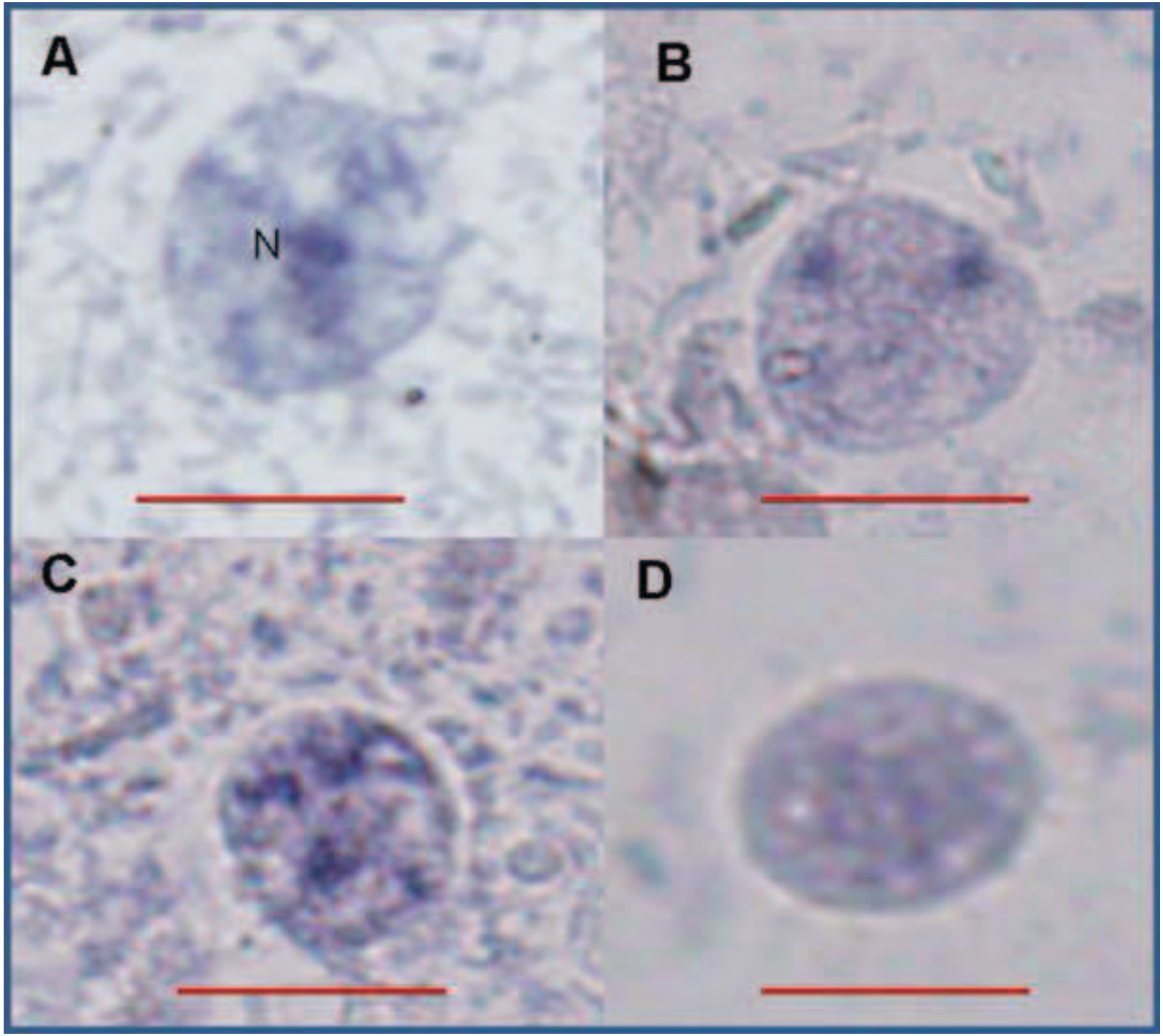

Figure 11
Click here to download high resolution image

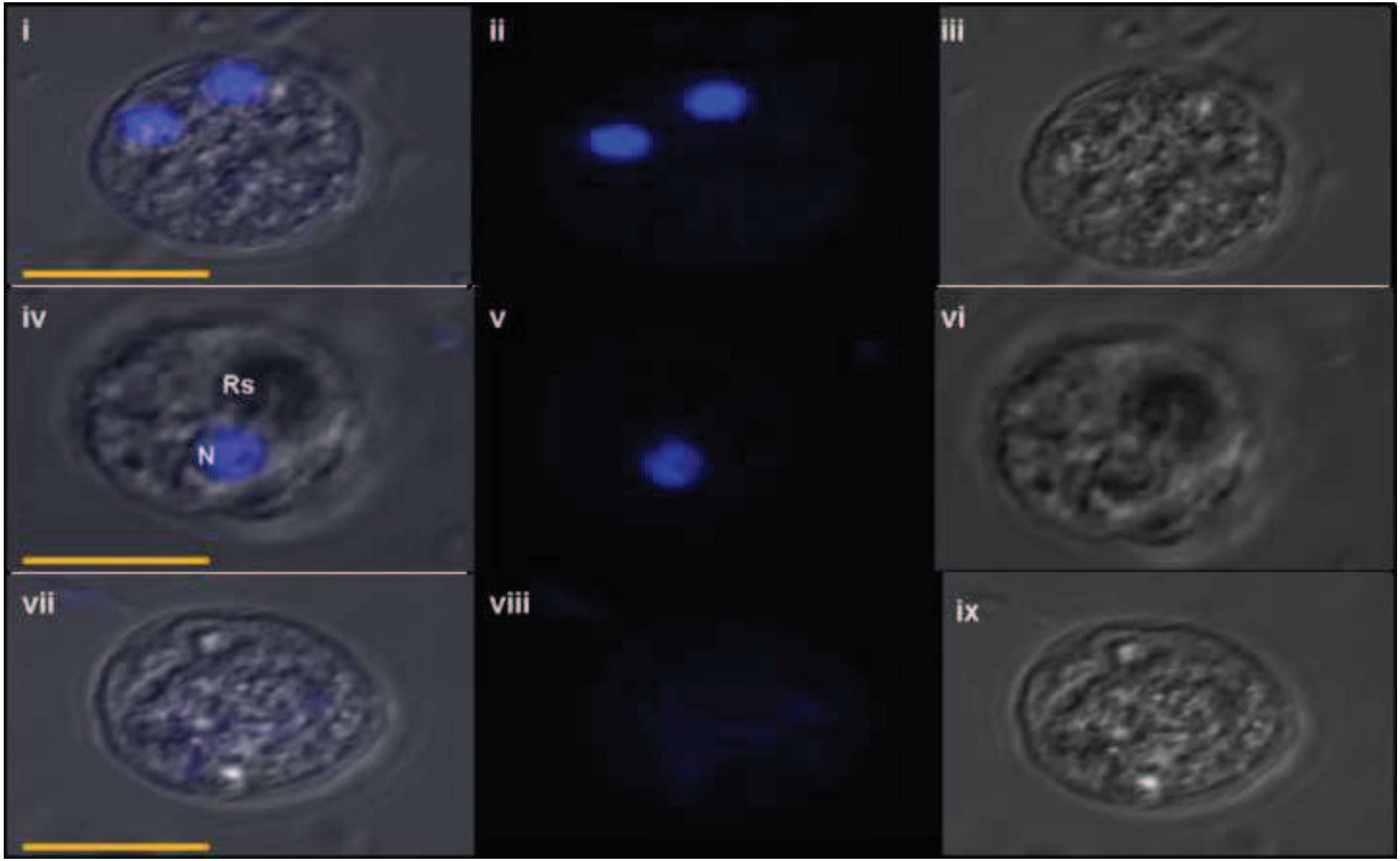

Figure 12
Click here to download high resolution image

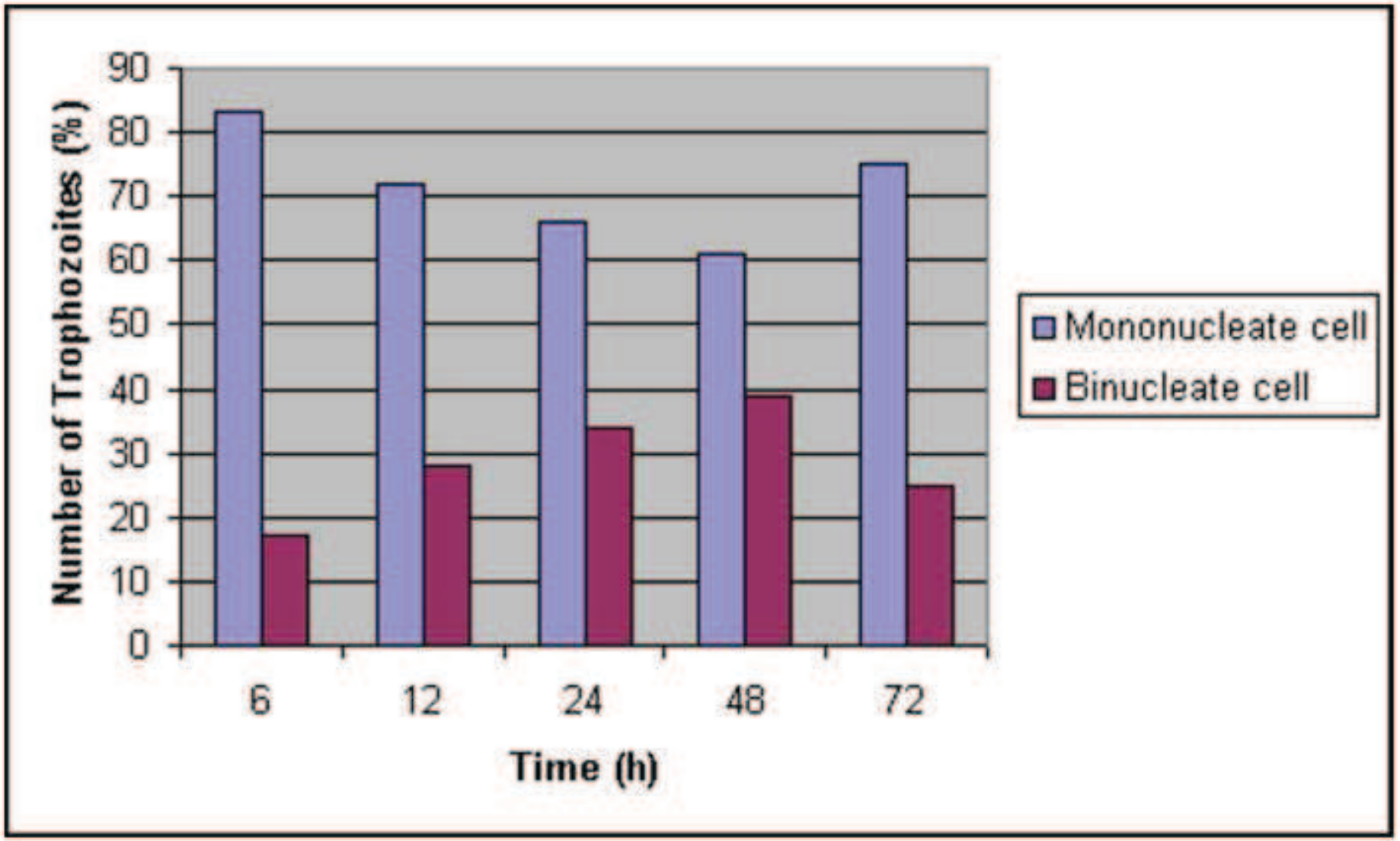

Figure 13
Click here to download high resolution image